Analysis-oriented stress-strain models for FRP-confined concrete

T. Jiang[1] and J.G. Teng[1,*]

[1]Department of Civil and Structural Engineering
The Hong Kong Polytechnic University, Hong Kong, China
*cejgteng@polyu.edu.hk

Abstract: Many stress-strain models have been developed for fibre-reinforced polymer (FRP)-confined concrete. These models fall into two categories: (a) design-oriented models in simple closed-form expressions for direct use in design; and (b) analysis-oriented models in which the stress-strain curve is generated via an incremental process. This paper is concerned with analysis-oriented models, and in particular, those models based on the commonly accepted approach in which a model for actively-confined concrete is used as the base model. The paper first provides a critical review and assessment of existing analysis-oriented models for FRP-confined concrete. For this assessment, a database of 48 recent tests conducted by the authors' group is presented; this database includes 23 new tests which have not previously been published. This assessment clarifies how each of the key elements forming such a model affects its accuracy and identifies a recent model proposed by the authors' group as being the most accurate. The paper then presents a refined version of this model, which provides more accurate predictions of the stress-strain behaviour, particularly for weakly-confined concrete.

Key words: FRP; confinement; concrete; dilation properties; stress-strain behaviour; stress-strain models

1 Introduction

Fibre-reinforced polymer (FRP) jackets have been widely used in practice as a confining material for concrete columns to achieve significant enhancements in both strength and ductility (Teng et al. 2002; De Lorenzis and Tepfers 2003; Wu et al. 2006). As the design of such jackets requires an accurate stress-strain model for the concrete they confine (FRP-confined concrete), extensive recent research has been carried out on the stress-strain behaviour of FRP-confined concrete, from which a number of stress-strain models have resulted. These models fall into two main categories: (1) design-oriented models and (2) analysis-oriented models. The former models are generally in closed-form equations directly derived from test results, treating FRP-confined concrete as a single "composite" material, and are thus simple and convenient to apply in design. By contrast, the latter models treat the FRP jacket and the concrete core separately, and predict the behaviour of FRP-confined concrete by an explicit account of the interaction between the FRP jacket and the confined concrete core via radial displacement compatibility and equilibrium conditions. Analysis-oriented models are more versatile and accurate in general, are often the preferred choice for use in more involved analysis than is required in design (e.g. nonlinear finite element analysis of concrete structures with FRP confinement), and are applicable/easily extendible to concrete confined with materials other than FRP. They can also be employed to generate numerical results for use in the development of a design-oriented model.

The confinement provided by an FRP jacket to a concrete core is passive rather than active, as the confining pressure from the jacket is induced by and increases with the expansion of

the concrete core. In most existing analysis-oriented models for FRP-confined concrete, a theoretical model for actively-confined concrete (i.e. the confining pressure is externally applied and remains constant as the axial stress increases), which is referred to as an active-confinement model for brevity hereafter, is employed as the base model; the axial stress-axial strain curve (simply referred to as the axial stress-strain curve or the stress-strain curve hereafter) of FRP-confined concrete is then generated through an incremental process, with the resulting stress-strain curve crossing a family of stress-strain curves for the same concrete under different levels of active confinement (Teng and Lam 2004). Models of Mirmiran and Shahawy (1996, 1997a), Spoelstra and Monti (1999), Fam and Rizkalla (2001), Chun and Park (2002), Harries and Kharel (2002), Marques et al. (2004), Binici (2005) and Teng et al. (2007a) are all of this type. Two other models (Harmon et al. 1998; Becque et al. 2003) adopted alternative approaches for modelling the concrete (Teng and Lam 2004). The first approach, in which an active-confinement model is used, has been much more popular than the other approaches as it leads to conceptually simple yet effective models. This paper is limited to analysis-oriented models developed through this approach. For a brief discussion of the models by Harmon et al. (1998) and Becque et al. (2003), the reader is referred to Teng and Lam (2004).

It should be noted that among those models with an active-confinement base model, the models of Spoelstra and Monti (1999), Fam and Rizkalla (2001), Chun and Park (2002), and Harries and Kharel (2002) have been briefly summarized and assessed through comparisons with test stress-strain curves of FRP-confined concrete with a significant level of confinement (dependent on the hoop membrane stiffness of the FRP jacket) so that the stress-strain curves are monotonically ascending. The present paper extends the work of Teng and Lam (2004) in the following aspects:

(a) apart from the four models mentioned above, the model of Mirmiran and Shahawy (1997a) together with three more recent models (Marques et al. 2004; Binici 2005 and Teng et al. 2007a) are also included in the critical review and assessment;
(b) a much more thorough assessment is presented for all these models by considering different levels of confinement covering both the ascending and descending types of stress-strain curves, with the emphasis being on the accuracy of the key elements of such models, including the lateral-to-axial strain relationship for FRP-confined concrete, as well as the stress-strain equation and the peak axial stress point of the active-confinement base model;
(c) new results from recent tests conducted by the authors' group are employed in the assessment and some of these tests are for FRP-confined concrete with a descending stress-strain curve (i.e. weakly-confined concrete) which is less well understood and for concrete with very strong FRP confinement which has received little attention in previous work.
(d) the lateral-to-axial strain relationship, which takes various forms and is essential to this type of models (Teng and Lam 2004), is thoroughly examined; and
(e) finally, a refined version of Teng et al.'s (2007a) model is presented to provide more accurate predictions, particularly for weakly-confined concrete.

2 Test database

2.1 General

A test database, containing the results of axial compression tests of 48 FRP-confined concrete cylinders (diameter D = 152 mm and height H = 305 mm), is employed herein to evaluate the

performance of existing analysis-oriented stress-strain models. All these tests have recently been conducted by the authors' group at The Hong Kong Polytechnic University, so the tests were conducted under standard conditions and all information required for evaluating stress-strain models can be readily and accurately extracted.

Among these 48 tests, 25 of them have been published (i.e. specimens 01 to 13 in Lam and Teng 2004; specimens 14 to 19 in Lam et al. 2006 and Specimens 20 to 25 in Teng et al. 2007b) and were used in developing Teng et al.'s (2007a) model, the other 23 tests are new tests that have never been published or used in developing any of the existing stress-strain models. The new tests significantly widened the range of confinement ratios from 0.08-0.46 for the 25 published tests to 0.07-0.99 for the 48 tests considered in this paper; some of the test stress-strain curves feature a descending branch while others are rapidly ascending. The confinement ratio $f_l / f_{co}^{'}$ refers to the ratio of the confinement pressure f_l at jacket rupture to the compressive strength of unconfined concrete $f_{co}^{'}$, with

$$f_l = \frac{2E_{frp} t \varepsilon_{h,rup}}{D} \tag{1}$$

where E_{frp} and t are the elastic modulus and the thickness of FRP jacket respectively, and $\varepsilon_{h,rup}$ is the hoop rupture strain of FRP jacket. In the present database, the maximum increase in concrete strength as a result of FRP confinement is about 320%. Further details of this test database are available in Table 1.

For ease of discussion, the terms "weakly-confined concrete", "moderately-confined concrete" and "heavily-confined concrete" are used herein. Weakly-confined concrete refers to concrete whose stress-strain curves feature a descending branch. Moderately-confined concrete and heavily-confined concrete both refer to concrete whose stress-strain curves are of the bi-linear ascending type. The latter two are differentiated using the $f_{cu}^{'} / f_{co}^{'}$ ratio, where $f_{cu}^{'}$ is the axial stress at ultimate axial strain of FRP-confined concrete. When $f_{cu}^{'} / f_{co}^{'} < 2$, the concrete is said to be moderately-confined, while all other cases with $f_{cu}^{'} / f_{co}^{'} \geq 2$ are said to be heavily-confined.

2.2 Specimens and instrumentation

The preparation of all 48 specimens followed a standard procedure, which has been described in Lam and Teng (2004). The FRP jackets were all formed via the wet lay-up process and all had hoop fibres only. For each batch of concrete, 2 or 3 control specimens of the same size were also tested, from which the average values of the compressive strength of unconfined concrete $f_{co}^{'}$ and the corresponding axial strain ε_{co} were found.

For each control specimen, two longitudinal strain gauges, with a gauge length of 120 mm covering the mid-height region, were placed at 180° apart to measure the axial strains. Two other strain gauges, with a gauge length of 60 mm, were placed at 180° apart to measure the hoop strains. For each FRP-confined specimen, either 6 or 8 unidirectional strain gauges, with a gauge length of 20 mm, were installed at mid-height to measure the hoop strains and another 2 strain gauges of the same type were installed at mid-height to measure the axial strains. In addition, axial strains were also measured by two linear variable displacement transducers (LVDTs) at 180° apart and covering the mid-height region of 120 mm for both

unconfined and confined specimens. All axial strains reported in this paper are the average values of readings from the two LVDTs.

Among the hoop strain gauges, 5 of them equally spaced at 45^o were located outside the 150 mm wide overlapping zone, from which the average hoop strain was found. The hoop strain readings within the overlapping zone are generally smaller than those elsewhere as the overlapping zone has a larger jacket thickness. These readings therefore reflect neither the actual strain capacity of the confining jacket nor the actual dilation properties of the confined concrete, and should thus be excluded when interpreting the behaviour of FRP-confined concrete (Lam and Teng 2004). It should be noted that such important processing of the hoop strain readings is not possible with existing tests reported by other researchers, for which the precise number and locations of strain gauges for measuring hoop strains are generally not reported.

Since the 48 tests were conducted within different research projects, there were some differences in the loading methods employed. Specimens 01 to 13 were tested with load control at a constant rate of 300kN/min, while all other specimens were tested with displacement control, at a constant rate of either 0.18 mm/min or 0.6 mm/min; both rates are acceptable for such tests. All test data, including the readings of the axial load, strain gauges and the LVDTs were collected with a data logger and simultaneously saved in a computer.

2.3 Test results

All the FRP-confined specimens were found to fail by the sudden rupture of the FRP jacket outside the overlapping zone. The key test results are given in Table 1. The compressive strength of confined concrete $f_{cc}^{'}$ was obtained by dividing the maximum load by the cross-sectional area of the specimen. Stress-strain curves of both the ascending and the descending types were captured. When the stress-strain curve is of the descending type, the axial stress at ultimate axial strain $f_{cu}^{'}$ is also reported in Table 1.

The stress-strain curves from all tests of the present database are shown in Fig. 1, where the lateral strains ε_l are shown on the left and the axial strains ε_c are shown on the right. Both the axial strain and the lateral strain are normalized by the corresponding value of ε_{co}, while the axial stress σ_c is normalized by the corresponding value of $f_{co}^{'}$. The following sign convention is adopted: in the concrete, compressive stresses and strains are positive, but in the FRP, tensile stresses and strains are positive. The predictions of the refined version of Teng et al.'s (2007a) model are also provided in Fig. 1. The predicted curves end at a hoop rupture strain averaged from either two or three physically identical specimens. The refinement of Teng et al.'s (2007a) model is discussed later in paper.

The pair of specimens 20 and 21 as well as the pair of specimens 28 and 29 showed a descending branch in their stress-strain curves and the compressive strengths of these specimens are only slightly higher than those of the unconfined specimens. These specimens were all confined with a one-ply GFRP jacket, and based on the experimental hoop rupture strains, the average confinement ratios of the two pairs are 0.079 and 0.067 respectively. By contrast, all other FRP-confined specimens shown in Fig. 1 exhibited the well-known bilinear stress-strain curve of the ascending type. It should be noted that the pair of specimens 42 and 43, which had a smaller confinement ratio than that of the pair of specimens 20 and 21, also

exhibited the ascending type stress-strain curve. This is because the elastic modulus of the FRP jacket of the former pair is much larger than that of the latter pair, indicating that the nature of the stress-strain curve depends not only on the confinement ratio but also on the stiffness of the jacket.

3 Existing analysis-oriented models for FRP-confined concrete

3.1 General concept

The concept of establishing a passive-confinement stress-strain model from an active-confinement base model through an incremental approach has previously been employed for steel-confined concrete by Ahmad and Shah (1982) and Madas and Elnashai (1992). The first documented attempt to extend this approach to FRP-confined concrete was made by Mirmiran and Shahawy (1996). This model follows the procedure proposed by Madas and Elnashai (1992). However, as some of its parameters are not clearly defined (Teng and Lam 2004), this model was not included in the assessment undertaken by Teng and Lam (2004) and is also not included in the present comparisons. A later version of this model proposed by the same authors (Mirmiran and Shahawy 1997a) does not specify the active-confinement base model and was thus also excluded from the assessment given in Teng and Lam (2004). In the present study, the model of Mander et al. (1988) is assumed as the active-confinement model for use in this later version, as this base model is employed in the earlier version of their model (Mirmiran and Shahawy 1996). Following the work of Mirmiran and Shahawy (1996, 1997a), a number of models of this kind have been proposed, including Spoelstra and Monti (1999), Fam and Rizkalla (2001), Chun and Park (2002), Harries and Kharel (2002), Marques et al. (2004), Binici (2005) and Teng et al. (2007a).

These models are all built on the assumption that the axial stress and the axial strain of concrete confined with FRP at a given lateral strain are the same as those of the same concrete actively confined with a constant confining pressure equal to that supplied by the FRP jacket (Teng et al. 2007a). This assumption is equivalent to assuming that the stress path of the confined concrete does not affect its stress-strain behaviour. As a result of this assumption, the stress-strain curve of FRP-confined concrete can be obtained through the following procedure:

(1) for a given axial strain, find the corresponding lateral strain according to the lateral-to-axial strain relationship;
(2) based on force equilibrium and radial displacement compatibility between the concrete core and the FRP jacket, calculate the corresponding lateral confining pressure provided by the FRP jacket;
(3) use the axial strain and the confining pressure obtained from steps (1) and (2) in conjunction with an active-confinement base model to evaluate the corresponding axial stress, leading to the identification of one point on the stress-strain curve of FRP-confined concrete; and
(4) repeat the above steps to generate the entire stress-strain curve. Fig. 2 illustrates the concept of this incremental approach.

It is not difficult to realise that in the above procedure, the key elements that determine the accuracy of the predictions are the active-confinement model and the lateral-to-axial strain relationship. The performance of the active-confinement model depends on: (a) the peak axial stress (i.e. failure surface) and the corresponding axial strain; and (b) the stress-strain equation. The lateral-to-axial strain relationship, which depicts the unique dilation property of

FRP-confined concrete, is either implicitly or explicitly given in existing models. An iterative procedure is required in steps (1) and (2) to determine the correct lateral strain that corresponds to the current axial strain.

In the remainder of this section, the existing models are reviewed in terms of the three key aspects: the stress-strain equation and the peak axial stress point of the active confinement model, and the lateral-to-axial strain relationship. The existing models are also summarized in Table 2.

3.2 Peak axial stress point

Peak axial stress

The peak axial stress on the stress-strain curve of actively-confined concrete is the compressive strength of such concrete and the peak stress equation defines the failure surface of such concrete. The models of Mirmiran and Shahawy (1997a), Spoelstra and Monti (1999), Fam and Rizkalla (2001) and Chun and Park (2002) directly employ the "five parameter" multiaxial failure surface given by Willam and Warnke (1975) to define the peak axial stress:

$$f_{cc}^{'*} = f_{co}^{'}\left(2.254\sqrt{1+7.94\frac{f_l}{f_{co}^{'}}}-2\frac{f_l}{f_{co}^{'}}-1.254\right) \tag{2}$$

where $f_{cc}^{'*}$ is the peak axial stress of concrete under a specific constant confining pressure f_l.

Of the other four models, Harries and Kharel (2002) adopted the following equation proposed by Mirmiran and Shahawy (1997b):

$$f_{cc}^{'*} = f_{co}^{'} + 4.269\, f_l^{0.587} \tag{3}$$

Marques et al. (2004) adopted the following equation proposed by Razvi and Saatcioglu (1999):

$$f_{cc}^{'*} = f_{co}^{'} + 6.7\, f_l^{0.83} \tag{4}$$

Binici (2005) employed the Leon-Pramono criterion (Pramono and Willam 1989), which reduces to Eq. 5 if the tensile strength of unconfined concrete is taken to be 0.1 times of its compressive strength.

$$f_{cc}^{'*} = f_{co}^{'}\left(\sqrt{1+9.9\frac{f_l}{f_{co}^{'}}}+\frac{f_l}{f_{co}^{'}}\right) \tag{5}$$

Teng et al. (2007a) proposed the following linear function to define the peak axial stress:

$$f_{cc}^{'*} = f_{co}^{'} + 3.5\, f_l \tag{6}$$

The above equations for the peak axial stress are compared in Fig. 3, showing large differences between each other.

Axial strain at peak axial stress

Except the model of Marques et al. (2004), all existing models employ the following equation initially proposed by Richart et al. (1928) to define the axial strain at peak axial stress:

$$\varepsilon_{cc}^{*} = \varepsilon_{co}\left[1+5\left(\frac{f_{cc}^{'*}}{f_{co}^{'}}-1\right)\right] \tag{7}$$

where ε_{co} and ε_{cc}^{*} are respectively the axial strains at $f_{co}^{'}$ and $f_{cc}^{'*}$. Marques et al. (2004)

used Eq. 7 for concrete with $f_{co}^{'} \le 40\,\text{MPa}$ but for concrete of higher strength, Eq. 7 was modified with a factor introduced by Razvi and Saatcioglu (1999) to account for the reduced effectiveness in the enhancement of axial strain for high strength concrete. In Fig. 4, the predictions from all models of the axial strain at peak axial stress are compared, where the differences stem from the different expressions for the peak axial stress.

3.3 Stress-strain equation

All models except those of Harries and Kharel (2002) and Binici (2005) employ the following equation originally proposed by Popovics (1973) and later adopted by Mander et al. (1988) for steel-confined concrete:

$$\frac{\sigma_c}{f_{cc}^{'*}} = \frac{\left(\varepsilon_c / \varepsilon_{cc}^{*}\right) r}{r - 1 + \left(\varepsilon_c / \varepsilon_{cc}^{*}\right)^r} \tag{8}$$

where the constant r is defined by

$$r = \frac{E_c}{E_c - f_{cc}^{'*} / \varepsilon_{cc}^{*}} \tag{9}$$

where E_c is the elastic modulus of concrete.

In the model of Harries and Kharel (2002), the stress-strain equation of actively-confined concrete described by Eq. 8 is modified by a factor which was introduced to control the slope of the descending branch. The model of Binici (2005) employs three separate expressions to describe the full stress-strain curve. The ascending branch is described using a linear expression followed by Eq. 8, while the descending branch is described using an exponential expression.

3.4 Lateral-to-axial strain relationship

The lateral-to-axial strain relationship, not available in an active-confinement model, provides the essential connection between the response of the concrete core and the response of the FRP jacket, in a passive-confinement model for FRP-confined concrete. This relationship has been established via different approaches, and is either explicitly stated or implicitly given.

Explicit lateral-to-axial strain relationships are used in the models of Mirmiran and Shahawy (1997a), Harries and Kharel (2002) and Teng et al. (2007a). Mirmiran and Shahawy (1997a) used the tangent dilation ratio μ_t (the absolute value of the tangent slope of the lateral-to-axial strain curve of FRP-confined concrete; i.e. $\mu_t = \left|\mathrm{d}\varepsilon_l / \mathrm{d}\varepsilon_c\right|$) to link the lateral strain and the axial strain. A fractional function was introduced by these authors to describe the tangent dilation ratio based on their own test results of FRP-confined concrete. Harries and Kharel (2002) instead used the secant dilation ratio μ_s (the absolute value of the secant slope of the lateral-to-axial strain curve of FRP-confined concrete; i.e. $\mu_s = \left|\varepsilon_l / \varepsilon_c\right|$), which is also based on their own test results of FRP-confined concrete, to relate the axial strain to the lateral strain. A simplified tri-linear equation was used to describe the variation of the secant dilation ratio. It should be noted that Harries and Kharel (2002) used different equations to predict the lateral strains of CFRP-confined and GFRP-confined concrete respectively. Based on a careful interpretation of the dilation properties of confined and unconfined concrete, Teng et al. (2007a) proposed the following lateral-to-axial strain equation that is applicable to

un-confined, actively confined and FRP-confined concrete:

$$\frac{\varepsilon_c}{\varepsilon_{co}} = 0.85\left(1+8\frac{\sigma_l}{f_{co}^{'}}\right)\left\{\left[1+0.75\left(\frac{-\varepsilon_l}{\varepsilon_{co}}\right)\right]^{0.7} - \exp\left[-7\left(\frac{-\varepsilon_l}{\varepsilon_{co}}\right)\right]\right\} \tag{10}$$

where σ_l is the confining pressure. In actively confined concrete, the concrete is subject to a constant confining pressure σ_l throughout the loading process, but in FRP-confined concrete, the passive lateral confining pressure depends on the stiffness of the FRP jacket and increases continuously with the hoop strain of FRP ε_h. For a given hoop/lateral strain, the confining pressure supplied by the FRP jacket is

$$\sigma_l = \frac{E_{frp} t \varepsilon_h}{R} = -\frac{E_{frp} t \varepsilon_l}{R} \tag{11}$$

Implicit lateral-to-axial strain relationships were adopted by other researchers. Spoelstra and Monti (1999) adopted the simple constitutive model proposed by Pantazopoulou and Mills (1995), which describes the decrease of secant modulus of concrete with an increasing area strain, to determine the lateral strain. Marques et al. (2004) employed a similar constitutive model, but they argued that the one used by Spoelstra and Monti (1999) does not ensure $\left(f_{co}^{'}, \varepsilon_{co}\right)$ corresponds to the peak point on the stress-strain curve of unconfined concrete. A coefficient was thus introduced to overcome this shortcoming. In the model of Fam and Rizkalla (2001), an equation representing the variation of secant dilation ratio with confining pressure was developed based on the results of Gardner (1969) from triaxial compression tests of concrete to determine the lateral strain. In the model of Chun and Park (2002), a cubic polynomial equation developed by Elwi and Murray (1979) based on the results of Kupfer et al. (1969) from uniaxial compression tests of concrete was used. In the model of Binici (2005), the secant dilation ratio was set to be a constant in the elastic stage, beyond which it was assumed to vary with the confining pressure.

4 Assessment of existing models

4.1 Test data

For the assessment of the accuracy of existing analysis-oriented stress-strain models in predicting the lateral strain-axial strain curve and the stress-strain curve, only comparisons with selected tests (specimens 28 and 29; 24 and 25; 34 and 35 in Table 1) are reported here due to space limitation. The observations made below are also supported by comparisons conducted using the remainder of the database not reported here.

The three sets of specimens correspond to confinement ratios of 0.067, 0.25, and 0.55 and $f_{cu}^{'}/f_{co}^{'}$ ratios of 0.88, 1.60, and 2.86 respectively to represent weakly-confined, moderately-confined and heavily-confined concrete. The comparisons focus on the dilation properties of FRP-confined concrete, although the full-range axial stress-strain behaviour is also examined. Following these comparisons, the ultimate axial strain and the corresponding axial stress from analysis-oriented models are also compared with the results of all 48 tests in the test database.

4.2 Dilation properties

It has been widely accepted that under axial compression, unconfined concrete experiences volumetric compaction up to 90% of the peak stress. Thereafter the concrete shows unstable volumetric dilation due to the rapidly increasing lateral-to-axial strain ratio. However, this lateral dilation can be effectively constrained by an FRP jacket (Lam and Teng 2003; Teng et al. 2007a). In FRP-confined concrete, this lateral dilation results in a continuously increasing lateral confining pressure provided by the FRP jacket. The dilation properties of FRP-confined concrete are reflected by its lateral-to-axial strain relationship. A more direct way to investigate the dilation properties of FRP-confined concrete is to examine the tangent dilation ratio or the secant dilation ratio.

Figs 5-7 show the experimental variations of lateral strain, tangent dilation ratio and secant dilation ratio as the axial strain increases and those from existing analysis-oriented stress-strain models. These test data allow the following observations to be made: (a) in the initial stage of deformation, the tangent dilation ratio/secant dilation ratio is almost constant and is very close to the secant dilation ratio of unconfined concrete; (b) afterwards, the tangent dilation ratio/secant dilation ratio gradually increases, and the FRP jacket is increasingly mobilized to confine the concrete; (c) a typical lateral-to-axial strain curve of FRP-confined concrete features an inflection point corresponding to the maximum value of the tangent dilation ratio.

The three sets of comparisons are for weakly-confined, moderately-confined, and heavily-confined concrete specimens respectively (Figs 5-7). Each set of comparisons includes four types of curves, being the lateral-to-axial strain curves, the tangent dilation ratio curves, the secant dilation ratio curves and the stress-strain curves. All curves terminate at the point when the average FRP hoop rupture strain from the corresponding pair of tests is reached. In plotting the test tangent dilation ratio, some of the data points were filtered out to remove disturbances from local fluctuations due to data resolutions of closely spaced readings.

From the comparisons, it can be seen that the existing models lead to rather different predictions. The models of Fam and Rizkalla (2001) and Binici (2005) do not predict an inflection point on the lateral-to-axial strain curve (i.e. the predicted tangent dilation ratio/secant dilation ratio continuously increases with the axial strain). For the other models, although they are capable of predicting the inflection point, the ultimate axial strain and the maximum values of the tangent dilation ratio and the secant dilation ratio are poorly predicted in most cases. Mirmiran and Shahawy (1997a) proposed that the maximum value of the tangent dilation ratio occurs when the axial strain reaches ε_{co}, however, the present test results show that the confining system cannot fully suppress lateral dilation at such an early stage. This point instead occurs at an axial strain of approximately $2\varepsilon_{co}$. In addition, the tangent dilation ratio predicted by Mirmiran and Shahawy's (1997a) model can be negative under heavy confinement. The predictions of Spoelstra and Monti's (1999) model and Marques et al.'s (2004) model show some similarity in shape and they predict initial values of the tangent dilation ratio and the secant dilation ratio which are much smaller than those obtained from tests. The model of Harries and Kharel (2002) is excluded from Fig. 7, since the predicted tangent dilation ratio and secant dilation ratio are unreasonably small. This shortcoming is due to their logarithmic equation for the ultimate secant dilation ratio, which results in negative values under heavy confinement. In addition, their definition of the ultimate secant dilation ratio is in doubt, since it only considers the effect of jacket stiffness, but ignores the

effects of specimen size and compressive strength of unconfined concrete. Chun and Park's (2002) model suffers from the same drawback. These authors also used a logarithmic equation, which may predict negative values, to determine the ultimate secant dilation ratio. The model of Teng et al. (2007a) is seen to be the most accurate one. This model provides the most accurate predictions of the ultimate axial strains in all three situations. Apart from the weakly-confined concrete specimens, the tangent dilation ratio and the secant dilation ratio are both accurately predicted by this model.

It may be noted that although some of the models predict the ultimate axial strain quite accurately in some cases, the shape of the lateral-to-axial strain curve is not correctly captured. Ideally, both the ultimate point and the shape of the lateral-to-axial strain curve should be accurately predicted. However, it is found that given the same ultimate point, the stress-strain curve can be closely predicted as long as the overall trend of the lateral-to-axial strain ratio can be reasonably but not necessarily accurately predicted. Taking Teng et al.'s (2007a) model as an example, Fig. 8 demonstrates that for both the ascending and descending types of stress-strain curves, even if the lateral-to-axial stain curve is simply described using a straight line, which is obviously incorrect but reasonably close to the predicted lateral-to-axial strain curve, the predicted stress-strain curves are only slightly affected. This indicates that local inaccuracy of the lateral-to-axial strain curve only leads to small deviations in the predicted stress-strain curve. The parameters used to generate Fig. 8 are summarized in Table 3.

4.3 Stress-strain curves

The axial stress-axial strain curves are shown in Figs 5(d), 6(d) and 7(d). It can be seen that for the weakly-confined and moderately-confined concrete specimens, all existing models overestimate the ultimate axial strain and the corresponding axial stress. However, for the heavily-confined concrete specimens, the performance of these models improves. Among them, the model of Teng et al. (2007a) is again seen to be the most accurate one. A significant deficiency of this model is that it overestimates the axial stress at ultimate axial strain for weakly-confined concrete and moderately-confined concrete, especially for the former. In Figure 5(d), this model fails to predict the post-peak descending branch.

4.4 Ultimate condition

Due to space limitation, only three sets of typical test results are compared with existing models in the preceding sub-sections. These comparisons are mainly concerned with the lateral-to-axial strain relationship, although the axial stress-strain curves are also discussed. An alternative way to assess the predicted stress-strain behaviour is to compare the predicted ultimate axial strains and the corresponding axial stresses with the test values, as shown in Figs 9 to 16, which allows a much large number of tests to be included in the comparison. It should be noted that in assessing the model of Harries and Kharel (2002), six specimens with the largest confinement ratios are not included for the reason mentioned earlier.

On the whole, most models give poor predictions for the ultimate axial strain, mainly because the accuracy of the predicted ultimate axial strains depends heavily on the accuracy of the lateral-to-axial strain equation, which needs improvement as shown earlier. The models of Mirmiran and Shahawy (1997a) and Teng et al. (2007a) are the better models in predicting the ultimate axial strain. For the axial stress at ultimate axial strain, the performance of all models except that of Harries and Kharel (2002) becomes much better, with the models of

Marques et al. (2004), Binici (2005) and Teng et al. (2007a) giving more accurate predictions. It is interesting to note that the models of Mirmiran and Shahawy (1997a), Spoelstra and Monti (1999), Fam and Rizkalla (2001) and Chun and Park (2003) show very similar performance in predicting the axial stress at ultimate axial strain. A common feature of these four models is that they all employ Eq. 2 to predict the peak axial stress of actively-confined concrete, which suggests that the use of Eq. 2, which is widely accepted for steel-confined concrete, in an active-confinement base model does not lead to an accurate passive-confinement model for FRP-confined concrete. The model of Harries and Kharel (2002) performs worst in predicting the axial stress at ultimate axial strain. This is also mainly due to the inappropriate definition of the peak axial stress in the base model. If a modified failure surface is used, this model will perform better (Teng and Lam 2004). Among all these models, Teng et al.'s (2007a) model provides the most accurate predictions for both the ultimate axial strain and its corresponding axial stress.

5 Refinement of Teng et al's model

From the comparisons presented in the above section, it is clear that Teng et al.'s (2007a) model is the most accurate of all existing models. This model correctly captures the unique dilation properties of FRP-confined concrete, which is central to models of this kind, and shows much better performance over the other models in predicting the ultimate condition. Nevertheless, this model still suffers from one significant deficiency: it overestimates the axial stress at ultimate axial strain for weakly confined concrete and to a lesser degree for moderately-confined concrete (Figs 5(d) and 6(d)). Teng et al. (2007a) noticed that their model overestimated the responses of some weakly-confined specimens and suggested that any future improvements to their model should be focused on very weakly confined concrete. This problem was not resolved by Teng et al. (2007a), primarily due to the insufficient information available on concrete with weak FRP confinement and the scatter of the relevant test data available then. This problem becomes more obvious when the model is compared with the more precise test data of the present test database. A refinement of this model to eliminate this deficiency is presented in the present section, so that stress-strain curves of the descending type can also be accurately predicted by this model.

To identify a way of refining Teng et al.'s (2007a) model, its key elements need to be screened for possible improvements. The stress-strain equation in the active-confinement base model of Teng et al. (2007a) is also commonly employed by other models for FRP-confined concrete and is not expected to be a source of error. Fig. 19 provides some evidence for the accuracy of Eq. 8 (Popovics's equation). The lateral-to-axial strain relationship proposed by Teng et al. (2007a) overestimates the axial strain at a given lateral strain for weakly-confined concrete, although it is accurate for moderately-confined and heavily-confined concrete. However, this overestimation of the axial strain for weakly-confined concrete is not the cause of inaccuracy in predicting the descending branch. Indeed, if this overestimation is corrected, the accuracy of the predicted stress-strain curve will further degrade. Given the limited number of tests available on weakly-confined concrete and the good overall performance of the lateral-to-axial strain equation proposed by Teng et al. (2007a) (Figs 5-7), it is difficult to propose improvements to or to justify any modifications of this equation. The definition of the peak point of the stress-strain curve in the base model is therefore believed to be the main source of error. In particular, for the axial strain at peak axial stress, Eq. 7 which was initially proposed by Richart et al. (1928), is employed by all models without any critical examination, although different equations (Eqs 2 to 6) have been proposed for the peak axial stress. As a result, the definition of the peak axial

stress and the corresponding axial strain are examined here to develop a more satisfactory stress-strain model for FRP-confined concrete.

To this end, test results from four recent studies (Imran and Pantazopoulou 1996; Ansari and Li 1998; Sfer et al. 2002 and Tan and Sun 2004) on actively-confined concrete were collected and analysed. Since the stress-strain behaviour of high strength concrete under active confinement is known to differ from that of normal strength concrete (Ansari and Li 1998), only test results of normal strength concrete ($f_{co}^{'}$ = 20 to 50 MPa) reported in the above four studies are included in the analysis [the 51.8 MPa series of Tan and Sun (2004) is also included]. The range of confinement ratios of these tests is from 0.04 to 0.91, which is very close to that of FRP-confined concrete in the current database. These active-confinement test results are given in Table 4.

5.1 Peak axial stress in the base model

The classical work on concrete under active confinement conducted by Richart et al. (1928) led to the following equation for the peak axial stress:

$$\frac{f_{cc}^{'*}}{f_{co}^{'}} = 1 + k_1 \frac{f_l}{f_{co}^{'}} \tag{12}$$

where k_1 is the confinement effectiveness coefficient and = 4.1. While a value of 4.1 for k_1 is commonly quoted, a wide range of other values has also been proposed by different researchers based on their own test data on actively-confined concrete (see Candappa et al. 2001). In Teng et al.'s (2007a) model, a value of 3.5 is used for k_1 (see Eq. 6), which was deduced from test results of FRP-confined concrete and is within the existing range of proposed values for k_1 (Candappa et al. 2001).

As shown in Fig. 17, the dotted line, representing Eq. 6 for the peak axial stress, agrees well with the test results. It is important to note that although Eq. 6 was deduced from test results of FRP-confined concrete, it does provide accurate predictions for the test data of actively-confined normal strength concrete.

5.2 Axial strain at peak axial stress in the base model

Richart et al. (1928) also suggested that the effectiveness in the enhancement of axial strain is around 5 times that in the enhancement of axial stress. Eq. 7 was thus proposed for the axial strain at peak axial stress. Substitution of Eq. 12 into Eq. 7 yields

$$\frac{\varepsilon_{cc}^{*}}{\varepsilon_{co}} = 1 + 5k_1 \frac{f_l}{f_{co}^{'}} \tag{13}$$

In the analysis-oriented stress-strain models assessed in the present paper, Eq. 13 is accepted without any modification, except Marques et al. (2004), although different equations were proposed for the peak axial stress. A more rational approach to predict the degree of strain enhancement is to separate it from the definition of the peak axial stress. That is, the relationship between the strain enhancement ratio $\varepsilon_{cc}^{*}/\varepsilon_{co}$ and the confinement ratio $f_l / f_{co}^{'}$ should be directly established from active-confinement test data.

Based on the test data shown in Fig. 18, the following nonlinear equation is proposed for the axial strain at peak axial stress:

$$\frac{\varepsilon_{cc}^{*}}{\varepsilon_{co}} = 1 + 17.5\left(\frac{\sigma_l}{f_{co}^{'}}\right)^{1.2} \tag{14}$$

Fig. 18 shows that Eq. 14 provides accurate predictions of ε_{cc}^{*} deduced from the test results of Lam et al. (2006) for specimens confined with a 0.33 mm thick CFRP jacket. In Fig. 18, the test values of ε_{cc}^{*} for actively-confined concrete at different confining pressures σ_l were deduced from the axial stresses σ_c and axial strains ε_c of FRP-confined specimens using Eqs 6, 8 and 9. It can also be seen that Eq. 14 provides reasonably close predictions of the test results of actively-confined concrete, given the wide scatter exhibited by these test results.

Eq. 14 is thus proposed to replace its counterpart in Teng et al.'s (2007a) original model which can be written as

$$\frac{\varepsilon_{cc}^{*}}{\varepsilon_{co}} = 1 + 17.5\left(\frac{\sigma_l}{f_{co}^{'}}\right) \tag{15}$$

Eq. 14 is compared with Eqs 2 to 6 in Fig. 4. It is interesting to note that Eq. 14 predicts a trend that is opposite to that of the other equations. Teng et al.'s (2007a) model with Eq. 15 replaced by Eq. 14 is referred to as the refined model.

It should be noted that the incorporation of Eq. 14 into the base model shifts the location of the peak point of the stress-strain curve and slightly modifies the overall shape of the stress-strain curve. Fig. 19 shows the test stress-strain curves of the first three tests by Ansari and Li (1998) in Table 4 as well as the stress-strain curves predicted using the original base model where the peak point is defined by Eqs 6 and 15 and using the modified base model where the peak point is defined by Eqs 6 and 14. These tests were chosen for comparison as the curves were clearly reported in the original paper and their peak stresses are similar to the predictions of Eq. 6, which enables a more reliable and direct comparison. It can be seen that the curves predicted using the modified base model as well as the original base model are both in reasonably close agreement with the test curves, considering the large scatter of test values of ε_{cc}^{*} shown in Fig .18. This indicates that the modified definition of the peak point is at least as valid as the original definition when judged on the basis of these test results.

Fig. 20 shows the predictions of the axial stress at ultimate axial strain of the modified model versus the test data. It can be seen that the overestimation by Teng et al.'s (2007a) original model of the axial stress at ultimate axial strain for weakly-confined and moderately-confined concrete (Fig. 16(b)) has been corrected while the prediction for heavily-confined concrete is only very slightly affected (Fig. 20). The advantage of the refined model over the original model in predicting the entire stress-strain curve is demonstrated for selected specimens (Figs 1(d) and 1(e)). In these figures, the end of each curve is provided with a symbol to indicate the group it belongs to for easy comparisons. The refined model is seen to perform much better than the original model for weakly-confined specimens. The difference between the original and refined models reduces as the hoop membrane stiffness of the FRP jacket increases (Figs 1(d) and 1(e)). Comparisons shown in Figs 1(a)-1(c) and 1(f)-1(h) between the refined model and the test data show that overall, the refined model provide accurate predictions.

In all comparisons with test data in this paper, the test values of $f_{co}^{'}$ and ε_{co} were used. The

elastic modulus E_c and the Poisson's ratio of unconfined concrete were either those specified in an individual model or taken to be $4730\sqrt{f_{co}^{'}}$ (MPa) and 0.2 if they are not specified in the model. For Binici's (2005) model, the compressive fracture energy was found from $G_{fc} = 8.8\sqrt{f_{co}^{'}}$ (G_{fc} in MPa/mm and $f_{co}^{'}$ in MPa) (Nakamura and Higai 2001) and the characteristic length of the specimen in the loading direction l_c was taken to be the specimen height (i.e. 305 mm).

Teng et al. (2007a) suggested that when test values of ε_{co} are not available, a value of 0.0022 should be used with their model. For more accurate predictions, it is proposed here that when the refined model is used to predict the behaviour of FRP-confined concrete, the following equation proposed by Popovics (1973) should be used unless a test value is available:

$$\varepsilon_{co} = 0.000937\sqrt[4]{f_{co}^{'}} \quad (f_{co}^{'} \text{ in MPa}) \tag{16}$$

6 Conclusions

This paper has presented a thorough assessment of the performance of eight existing analysis-oriented stress-strain models for FRP-confined concrete which employ an active-confinement model as the base model, leading to the identification of Teng et al.'s (2007a) model as the most accurate through this assessment. A refined version of Teng et al.'s (2007a) model has also been proposed. The comparisons and discussions presented in this paper allow the following conclusions to be drawn:

1) The lateral-to-axial strain relationship, which reflects the unique dilation properties of FRP-confined concrete, is central to models of this kind. A successful model should accurately predict this relationship. Nevertheless, provided the overall trend of this relationship is reasonably well described, the axial stress-strain curve can be closely predicted, even if local inaccuracies exist in the lateral-to-axial strain equation;
2) The definitions of the peak axial stress and the corresponding axial strain in the active-confinement base model are also important to ensure the accuracy of an analysis-oriented model for FRP-confined concrete;
3) Most of the eight models examined in this paper correctly capture the dilation properties of FRP-confined concrete, but provide poor predictions of the ultimate axial strain. Their performance in predicting the axial stress at ultimate axial strain is however much better. The accuracy of the predicted ultimate axial strain depends mainly on the accuracy of the lateral-to-axial strain equation, while that of the predicted axial stress at ultimate axial strain depends mainly on the definitions of the peak axial stress and its corresponding strain in the base model.
4) The model of Teng et al. (2007a) performs the best among the eight models examined in this paper. This model provides accurate predictions of both the lateral-axial strain relationship and the ultimate condition, except that it overestimates the axial stress at ultimate axial strain for weakly-confined and to a lesser extent for moderately-confined concrete. As a result, its predictions are likely to be inaccurate for stress-strain curves with a descending branch.
5) The performance of the model of Teng et al. (2007a) for weakly-confined concrete can be significantly improved by replacing its equation for the strain at peak axial stress with a nonlinear equation proposed in this paper.

Acknowledgements

The authors are grateful for the financial support received from the Research Grants Council of the Hong Kong SAR (Project No: PolyU 5059/02E) and The Hong Kong Polytechnic University (Project Codes: RG88 and BBZH). The authors are also grateful to Dr. Lik Lam for his valuable assistance and to Dr. B. Binici for answering our queries on the implementation of his stress-strain model.

References

Ahmad, S.H. and Shah, S.P. (1982). "Stress-strain curves of concrete confined by spiral reinforcement", *ACI Journal*, 79(6): 484-490.

Ansari, F. and Li, Q.B. (1998). "High-strength concrete subjected to triaxial compression", *ACI Materials Journal*, 95(6): 747-755.

Becque, J., Patnaik, A.K. and Rizkalla, S.H. (2003). "Analytical models for concrete confined with FRP tubes", *Journal of Composites for Construction*, ASCE, 7(1): 31-38.

Binici, B. (2005). "An analytical model for stress–strain behavior of confined concrete", *Engineering Structures*, 27(7): 1040-1051.

Candappa, D.C., Sanjayan, J.G. and Setunge, S. (2001). "Complete triaxial stress-strain curves of high-strength concrete", *Journal of Materials in Civil Engineering*, ASCE, 13(3): 209-215.

Chun, S.S. and Park, H.C. (2002). "Load carrying capacity and ductility of RC columns confined by carbon fiber reinforced polymer." *Proceedings, 3rd International Conference on Composites in Infrastructure* (CD-Rom), University of Arizona, San Francisco, USA.

De Lorenzis, L. and Tepfers, R. (2003). "Comparative study of models on confinement of concrete cylinders with fiber-reinforced polymer composites", *Journal of Composites for Construction*, ASCE, 7(3): 219-237.

Elwi, A.A. and Murray, D.W. (1979). "A 3D hypoelastic concrete constitutive relationship", *Journal of the Engineering Mechanics Division*, ASCE, 105(4): 623-641.

Fam, A.Z. and Rizkalla, S.H. (2001). "Confinement model for axially loaded concrete confined by circular fiber-reinforced polymer tubes", *ACI Structural Journal*, 98(4): 451-461.

Gardner, N.J. (1969). "Triaxial behavior of concrete", *ACI Journal*, 66(2): 136-146.

Harmon, T.G., Ramakrishnan S. and Wang, E.H. (1998). "Confined concrete subjected to uniaxial monotonic loading", *Journal of Engineering Mechanics*, ASCE, 124(12): 1303-1308.

Harries, K.A. and Kharel, G. (2002). "Behavior and modeling of concrete subject to variable confining pressure", *ACI Materials Journal*, 99(2): 180-189.

Imran, I. and Pantazopoulou, S.J. (1996). "Experimental study of plain concrete under triaxial

stress", *ACI Materials Journal*, 93(6): 589-601.

Kupfer, H.B., Hilsdorf, H.K. and Rusch, H. (1969). "Behavior of concrete under biaxial stresses", *ACI Journal*, 66(8): 656-666.

Lam, L. and Teng, J.G. (2003). "Design-oriented stress-strain model for FRP-confined concrete", *Construction and Building Materials*, 17(6-7): 471-489.

Lam, L. and Teng, J.G. (2004). "Ultimate condition of fiber reinforced polymer-confined concrete", *Journal of Composites for Construction*, ASCE, 8(6): 539-548.

Lam, L., Teng, J.G., Cheung, C.H. and Xiao, Y. (2006). "FRP-confined concrete under axial cyclic compression", *Cement and Concrete Composites*, 28(10): 949-958.

Madas, P. and Elnashai, A.S. (1992). "A new passive confinement model for the analysis of concrete structures subjected to cyclic and transient dynamic loading", *Earthquake Engineering and Structural Dynamics*, 21(5): 409-431.

Mander, J.B., Priestley, M.J.N. and Park, R. (1988). "Theoretical stress-strain model for confined concrete", *Journal of Structural Engineering*, ASCE, 114 (8): 1804-1826.

Marques, S.P.C. Marques, D.C.S.C., da Silva J.L. and Cavalcante, M.A.A. (2004). "Model for analysis of short columns of concrete confined by fiber-reinforced polymer", *Journal of Composites for Construction*, ASCE, 8(4): 332-340.

Mirmiran, A. and Shahawy, M. (1996). "A new concrete-filled hollow FRP composite column", *Composites Part B-Engineering*, 27(3-4): 263-268.

Mirmiran, A. and Shahawy, M. (1997a). "Dilation characteristics of confined concrete", *Mechanics of Cohesive-Frictional Materials*, 2(3): 237-249.

Mirmiran, A. and Shahawy, M. (1997b). "Behavior of concrete columns confined by fiber composites", *Journal of Structural Engineering*, ASCE, 123(5): 583-590.

Nakamura, H. and Higai, T. (2001). "Compressive fracture energy and fracture zone length of concrete." *Modeling of Inelastic Behavior of RC Structures Under Seismic Loads*, Edited by P.B. Shing, T. Tanabe, ASCE: 471-487.

Popovics, S. (1973). "Numerical approach to the complete stress-strain relation for concrete", *Cement and Concrete Research*, 3(5): 583-599.

Pantazopoulou, S.J. and Mills, R.H. (1995). "Microstructural aspects of the mechanical response of plain concrete", *ACI Materials Journal*, 92(6): 605-616.

Pramono, E. and Willam K. (1989). "Fracture-energy based plasticity formulation of plain concrete", *Journal of Engineering Mechanics*, ASCE, 115(6): 1183-1204.

Razvi, S. and Saatcioglu, M. (1999). "Confinement model for high-strength concrete", *Cement and Concrete Research*, 125(3): 281-289.

Richart, F.E., Brandtzaeg, A. and Brown, R.L. (1928). *A Study of the Failure of Concrete under Combined Compressive Stresses*, Engineering Experiment Station, University of

Illinois, Urbana, U.S.A.

Sfer, D., Carol, I., Gettu, R. and Etse, G. (2002). “Study of the behavior of concrete under traxial compression”, *Journal of Engineering Mechanics*, ASCE, 128(2): 156-163.

Spoelstra, M.R. and Monti, G. (1999). “FRP-confined concrete model”, *Journal of Composites for Construction*, ASCE, 3(3): 143-150.

Tan, K.H. and Sun, X. (2004). “Failure criteria of concrete under triaxial compression”, *Proceedings, International Symposium on Confined Concrete* (CD-Rom), Changsha, China, 12-14 June.

Teng, J.G., Chen, J.F., Smith, S.T. and Lam, L. (2002). *FRP-Strengthened RC Structures*, John Wiley and Sons Ltd, UK.

Teng, J.G. and Lam, L. (2004). “Behavior and modeling of fiber reinforced polymer-confined concrete”, *Journal of Structural Engineering*, ASCE, 130(11): 1713-1723.

Teng, J.G., Huang, Y.L. Lam. L and Ye L.P. (2007a). “Theoretical model for fiber reinforced polymer-confined concrete”, *Journal of Composites for Construction*, ASCE, 11(2).

Teng, J.G., Yu, T. Wong, Y.L. and Dong, S.L. (2007b). “Hybrid FRP-concrete-steel tubular columns: concept and behaviour”, *Construction and Building Materials*, 21(4): 846-854.

Willam, K.J. and Warnke, E.P. (1975). “Constitutive model for the triaxial behaviour of concrete”, *Proceedings, International Association for Bridge and Structural Engineering*, 19: 1-30.

Wu, Y.F., Liu, T. and Oehlers, D.J (2006). “Fundamental principles that govern retrofitting of reinforced concrete columns by steel and FRP jacketing”, *Advances in Structural Engineering* 9(4): 507-533.

Table 1 Test database of FRP-confined concrete cylinders

Source	*Specimen*	*D* (mm)	*H* (mm)	$f_{co}^{'}$ (MPa)	ε_{co} (%)	*Fiber type*	*t* (mm)	E_{frp} (GPa)	$\varepsilon_{h,rup}$ (%)	$f_{cc}^{'}$ ($f_{cu}^{'}$) (MPa)	ε_{cu} (%)
Lam and Teng (2004)	1	152	305	35.9	0.203	Carbon	0.165	250.5	0.969	47.2	1.106
	2	152	305	35.9	0.203	Carbon	0.165	250.5	0.981	53.2	1.292
	3	152	305	35.9	0.203	Carbon	0.165	250.5	1.147	50.4	1.273
	4	152	305	35.9	0.203	Carbon	0.33	250.5	0.949	71.6	1.85
	5	152	305	35.9	0.203	Carbon	0.33	250.5	0.988	68.7	1.683
	6	152	305	35.9	0.203	Carbon	0.33	250.5	1.001	69.9	1.962
	7	152	305	34.3	0.188	Carbon	0.495	250.5	0.799	82.6	2.046
	8	152	305	34.3	0.188	Carbon	0.495	250.5	0.884	90.4	2.413
	9	152	305	34.3	0.188	Carbon	0.495	250.5	0.968	97.3	2.516
	10	152	305	38.5	0.223	Glass	1.27	21.8	1.440	51.9	1.315
	11	152	305	38.5	0.223	Glass	1.27	21.8	1.890	58.3	1.459
	12	152	305	38.5	0.223	Glass	2.54	21.8	1.670	77.3	2.188
	13	152	305	38.5	0.223	Glass	2.54	21.8	1.760	75.7	2.457
Lam et al. (2006)	14	152	305	41.1	0.256	Carbon	0.165	250	0.810	52.6	0.900
	15	152	305	41.1	0.256	Carbon	0.165	250	1.080	57.0	1.210

Lam et al. (2006)	16	152	305	41.1	0.256	Carbon	0.165	250	1.070	55.4	1.110
	17	152	305	38.9	0.250	Carbon	0.33	247	1.060	76.8	1.910
	18	152	305	38.9	0.250	Carbon	0.33	247	1.130	79.1	2.080
	19	152	305	38.9	0.250	Carbon	0.33	247	0.790	65.8	1.250
Teng et al. (2007b)	20	152	305	39.6	0.263	Glass	0.17	80.1	1.869	41.5 (38.8)	0.825
	21	152	305	39.6	0.263	Glass	0.17	80.1	1.609	40.8 (37.2)	0.942
	22	152	305	39.6	0.263	Glass	0.34	80.1	2.040	54.6	2.130
	23	152	305	39.6	0.263	Glass	0.34	80.1	2.061	56.3	1.825
	24	152	305	39.6	0.263	Glass	0.51	80.1	1.955	65.7	2.558
	25	152	305	39.6	0.263	Glass	0.51	80.1	1.667	60.9	1.792
Present study	26	152	305	33.1	0.309	Glass	0.17	80.1	2.080	42.4	1.303
	27	152	305	33.1	0.309	Glass	0.17	80.1	1.758	41.6	1.268
	28	152	305	45.9	0.243	Glass	0.17	80.1	1.523	48.4 (40.5)	0.813
	29	152	305	45.9	0.243	Glass	0.17	80.1	1.915	46.0 (40.5)	1.063
	30	152	305	45.9	0.243	Glass	0.34	80.1	1.639	52.8	1.203
	31	152	305	45.9	0.243	Glass	0.34	80.1	1.799	55.2	1.254
	32	152	305	45.9	0.243	Glass	0.51	80.1	1.594	64.6	1.554

Present study	33	152	305	45.9	0.243	Glass	0.51	80.1	1.940	65.9	1.904
	34	152	305	38.0	0.217	Carbon	0.68	240.7	0.977	110.1	2.551
	35	152	305	38.0	0.217	Carbon	0.68	240.7	0.965	107.4	2.613
	36	152	305	38.0	0.217	Carbon	1.02	240.7	0.892	129.0	2.794
	37	152	305	38.0	0.217	Carbon	1.02	240.7	0.927	135.7	3.082
	38	152	305	38.0	0.217	Carbon	1.36	240.7	0.872	161.3	3.700
	39	152	305	38.0	0.217	Carbon	1.36	240.7	0.877	158.5	3.544
	40	152	305	37.7	0.275	Carbon	0.11	260	0.935	48.5	0.895
	41	152	305	37.7	0.275	Carbon	0.11	260	1.092	50.3	0.914
	42	152	305	44.2	0.260	Carbon	0.11	260	0.734	48.1	0.691
	43	152	305	44.2	0.260	Carbon	0.11	260	0.969	51.1	0.888
	44	152	305	44.2	0.260	Carbon	0.22	260	1.184	65.7	1.304
	45	152	305	44.2	0.260	Carbon	0.22	260	0.938	62.9	1.025
	46	152	305	47.6	0.279	Carbon	0.33	250.5	0.902	82.7	1.304
	47	152	305	47.6	0.279	Carbon	0.33	250.5	1.130	85.5	1.936
	48	152	305	47.6	0.279	Carbon	0.33	250.5	1.064	85.5	1.821

Table 2 Summary of existing analysis-oriented models for FRP-confined concrete

Model	*Stress-strain Equation*	*Peak Point*		*Lateral-to-Axial Strain Relationship*
		Stress	*Strain*	
Mirmiran and Shahawy (1997a)	Popovics (1973)	Eq. 2	Eq. 7	Explicit, Mirmiran and Shahawy (1997a)
Spoelstra and Monti (1999)	Popovics (1973)	Eq. 2	Eq. 7	Implicit, Pantazopoulou and Mills (1995)
Fam and Rizkalla (2001)	Popovics (1973)	Eq. 2	Eq. 7	Implicit, Fam and Rizkalla (2001)
Chun and Park (2002)	Popovics (1973)	Eq. 2	Eq. 7	Implicit, Elwi and Murray (1979)
Harries and Kharel (2002)	Modified from Popovics (1973)	Eq. 3	Eq. 7	Explicit, Harries and Kharel (2002)
Marques et al. (2004)	Popovics (1973)	Eq. 4	Modified from Eq. 7	Implicit, Pantazopoulou and Mills (1995)
Binici (2005)	Modified from Popovics (1973)	Eq. 5	Eq. 7	Implicit, Binici (2005)
Teng et al. (2007a)	Popovics (1973)	Eq. 6	Eq. 7	Explicit, Eq. 10 Teng et al. (2007a)

Table 3 Summary of parameters used for generating Fig. 8

Figure No.	D (mm)	$f_{co}^{'}$ (MPa)	ε_{co} (%)	t (mm)	E_{frp} (GPa)	$\varepsilon_{h,rup}$ (%)
Fig. 8a	152	40	0.22	0.1	80	1.5
Fig. 8b	152	40	0.22	0.6	80	1.5

Table 4 Test results of concrete under active confinement

Source	$f_{co}^{'}$ (MPa)	ε_{co} (%)	f_l (MPa)	$f_l / f_{co}^{'}$	$f_{cc}^{'*}$ (MPa)	ε_{cc}^{*} (%)
Imran and Pantazopoulou (1996)	28.6	0.260	1.05	0.037	33.6	0.470
	28.6	0.260	2.1	0.073	36.4	0.675
	28.6	0.260	4.2	0.147	48.1	1.385
	28.6	0.260	8.4	0.294	65.2	2.375
	28.6	0.260	14.7	0.514	92.3	3.425
	28.6	0.260	21.0	0.734	114.5	4.460
	47.4	0.280	2.15	0.045	57.7	0.430
	47.4	0.280	4.3	0.091	67.3	0.690
	47.4	0.280	8.6	0.181	83.6	1.460
	47.4	0.280	17.2	0.363	118.1	2.530
	47.4	0.280	30.1	0.635	161.1	3.600
	47.4	0.28	43.0	0.907	204.7	4.730
Ansari and Li (1998)	47.2	0.202	8.3	0.176	79.7	1.349
	47.2	0.202	16.5	0.351	109.7	1.568
	47.2	0.202	24.8	0.527	130.7	2.049
	47.2	0.202	33.1	0.702	144.2	2.420
	47.2	0.202	41.4	0.878	166.9	2.950
Sfer et al. (2002)	32.8	0.180	1.5	0.046	45.5	0.260
	32.8	0.180	4.5	0.137	55.3	0.410
	32.8	0.180	9.0	0.274	65.7	0.830
	38.8	0.210	1.5	0.039	47.8	0.340
	38.8	0.210	4.5	0.116	58.2	0.520
	38.8	0.210	9.0	0.232	66.5	0.630
Tan and Sun (2004)	27.2	0.182	1.875	0.069	36.2	0.300
	27.2	0.182	1.875	0.069	35.7	0.289
	27.2	0.182	7.5	0.276	50.1	0.435

Tan and Sun (2004)	27.2	0.182	7.5	0.276	47.5	0.573
	27.2	0.182	15.0	0.551	72.1	0.744
	27.2	0.182	15.0	0.551	66.6	0.802
	51.8	0.238	1.875	0.036	64.8	0.329
	51.8	0.238	1.875	0.036	66	0.386
	51.8	0.238	7.5	0.145	86.6	0.456
	51.8	0.238	7.5	0.145	84.2	0.489
	51.8	0.238	12.5	0.241	99.3	0.492
	51.8	0.238	12.5	0.241	103.3	0.662

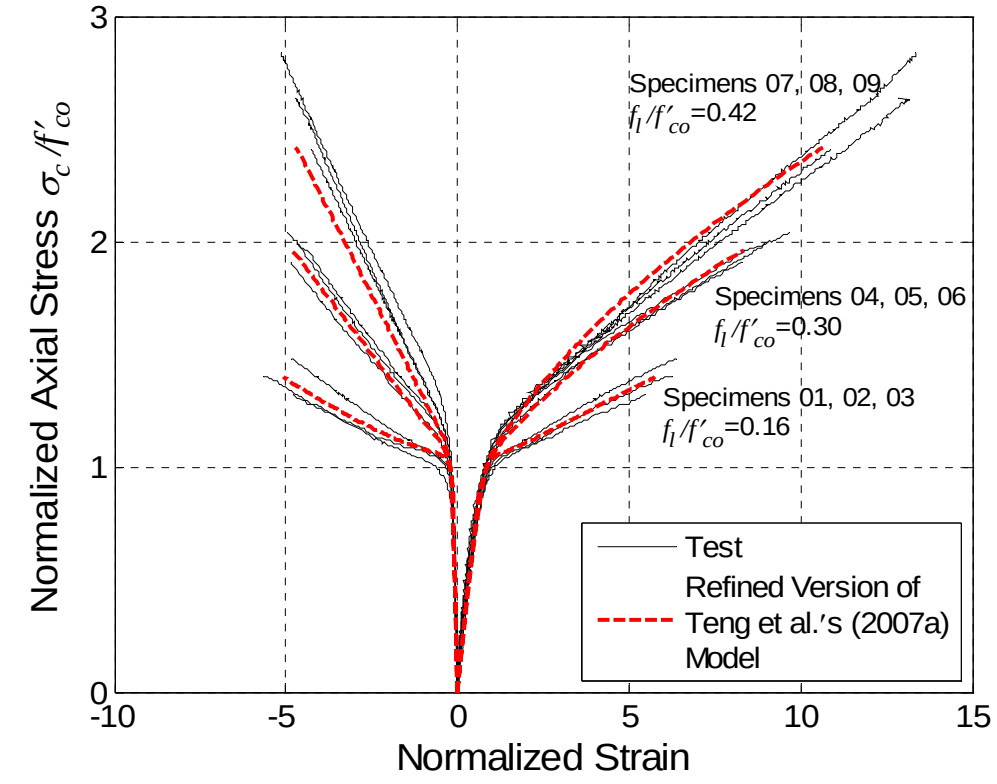

(a) Specimens 01 to 09

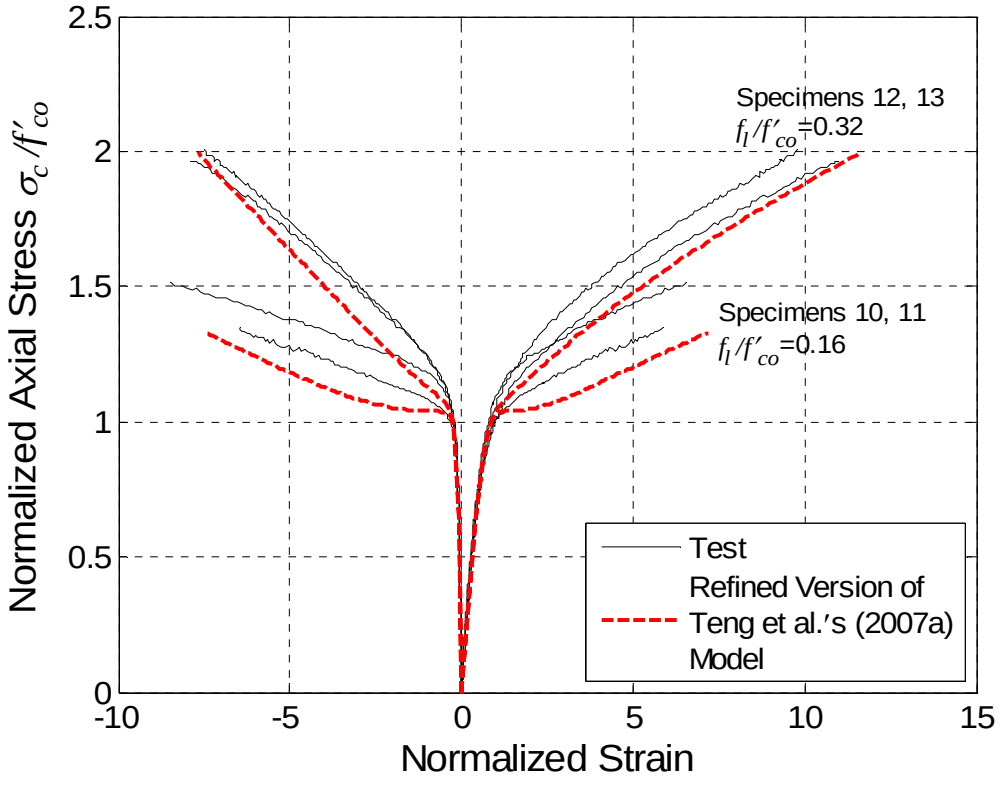

(b) Specimens 10 to 13

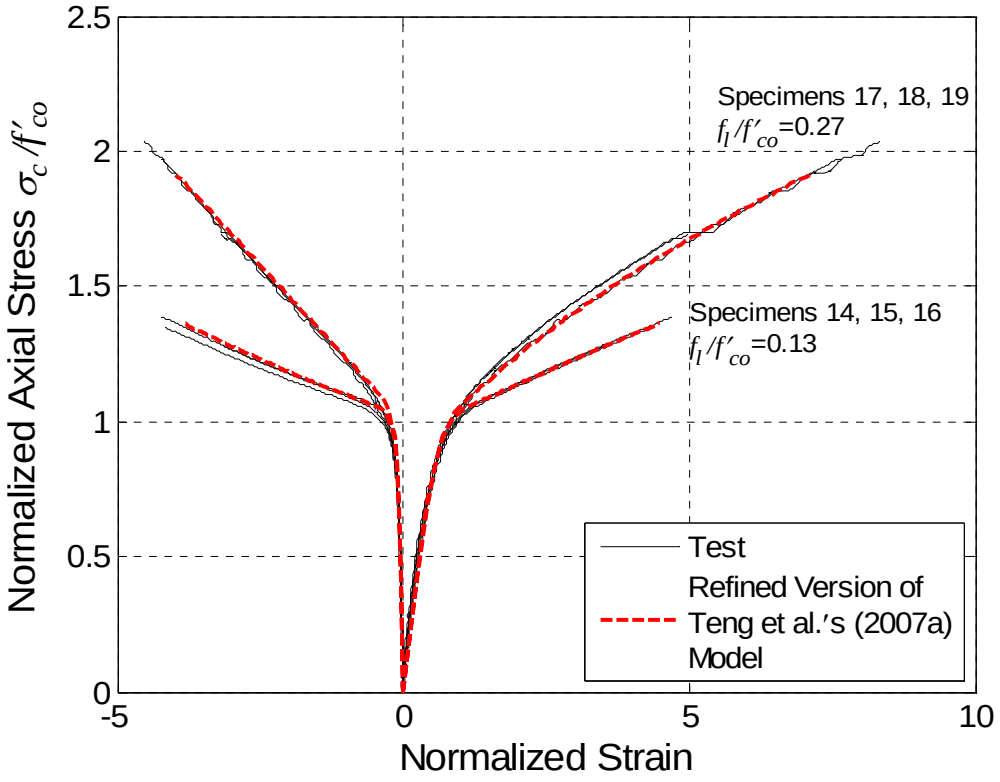

(c) Specimens 14 to 19

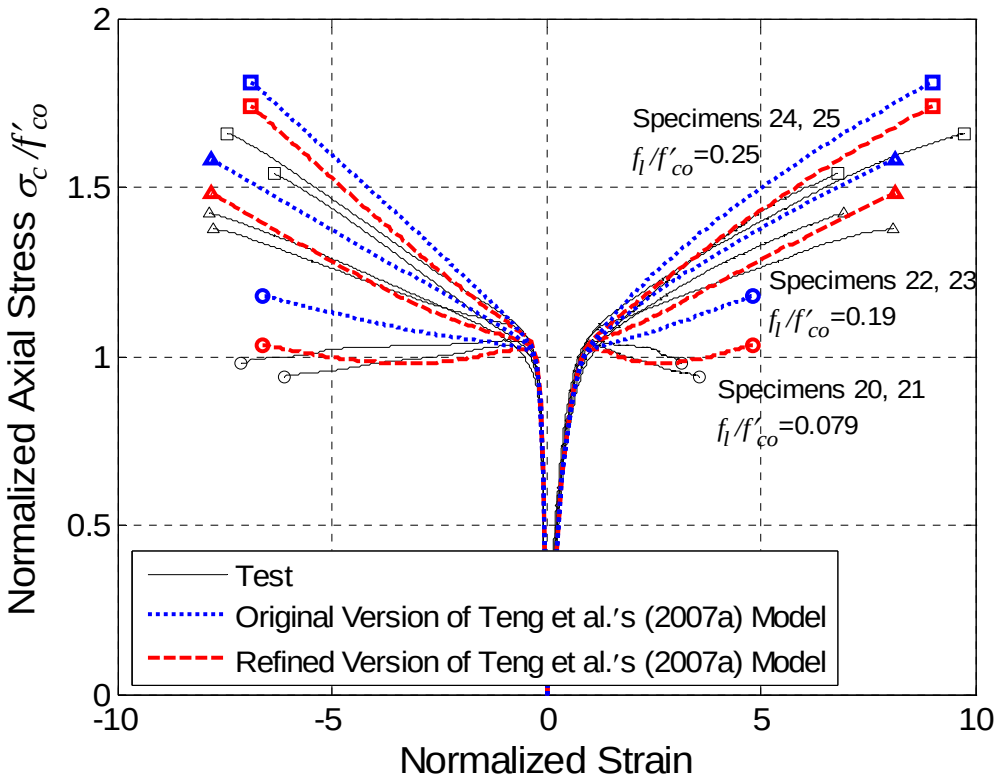

(d) Specimens 20 to 25

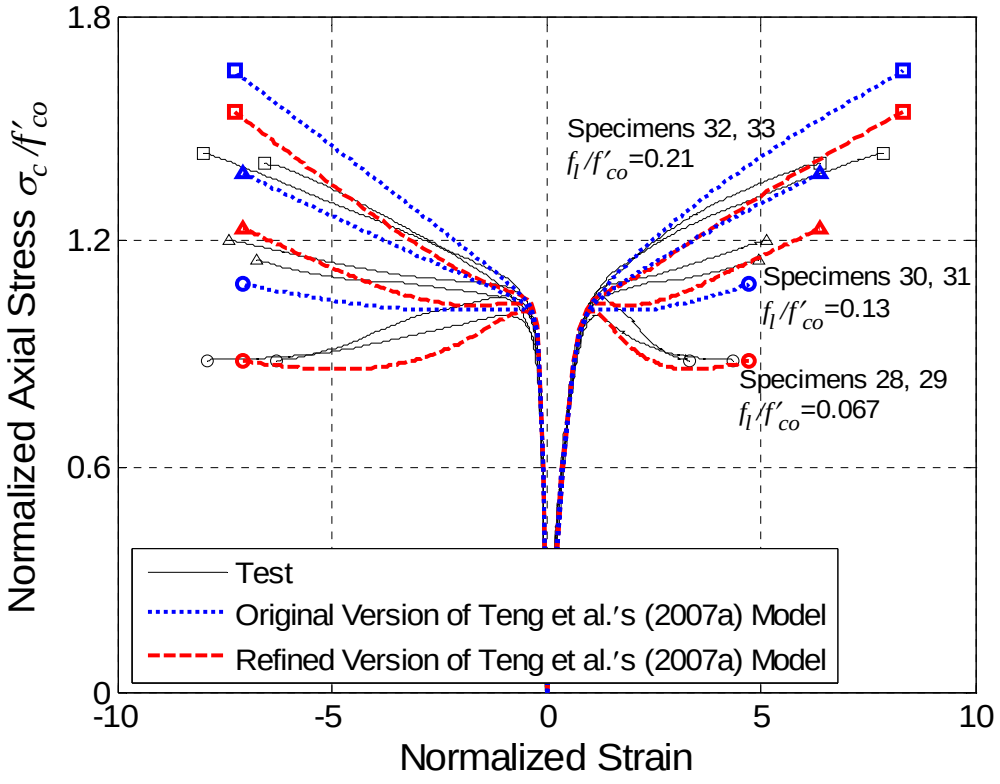

(e) Specimens 28 to 33

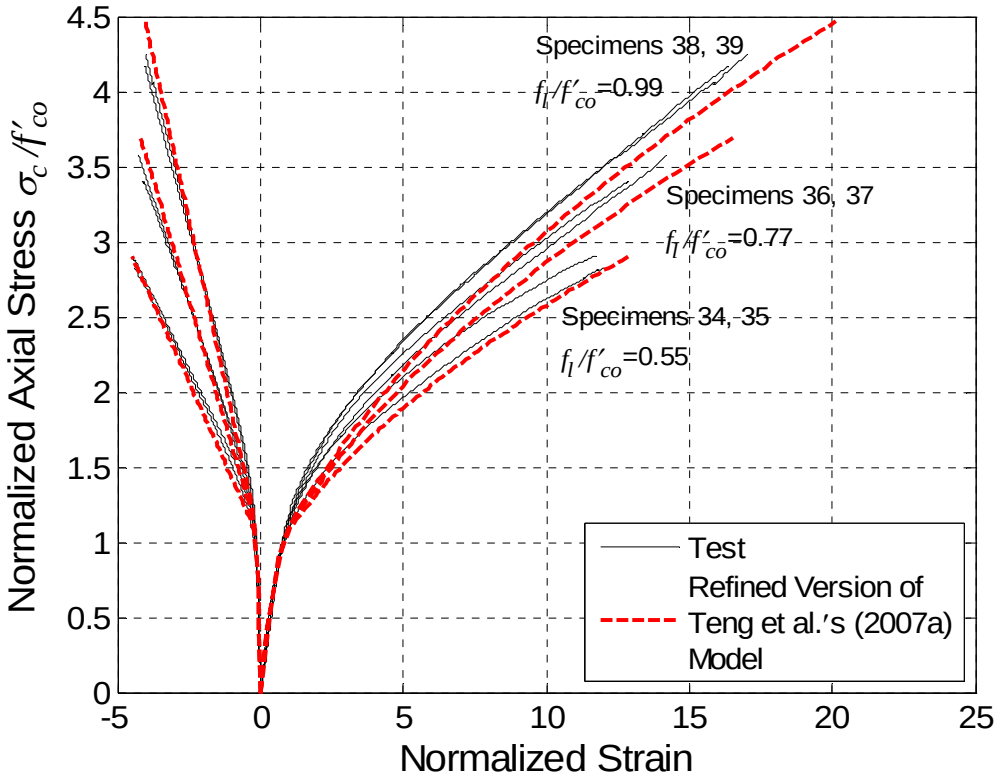

(f) Specimens 34 to 39

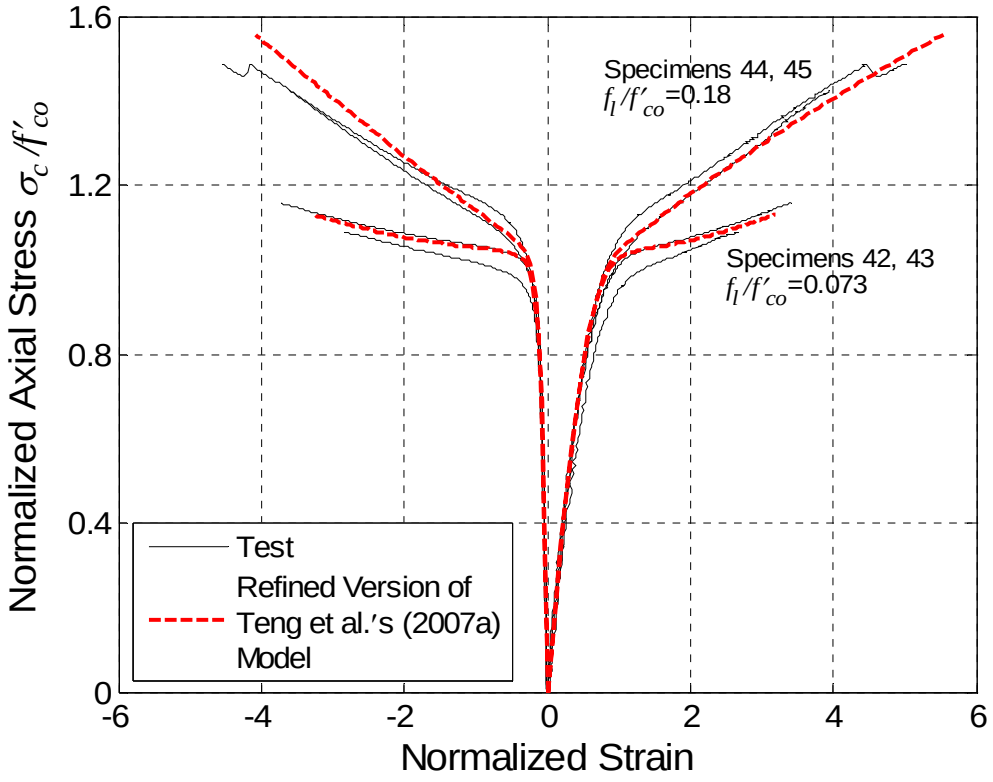

(g) Specimens 42to 45

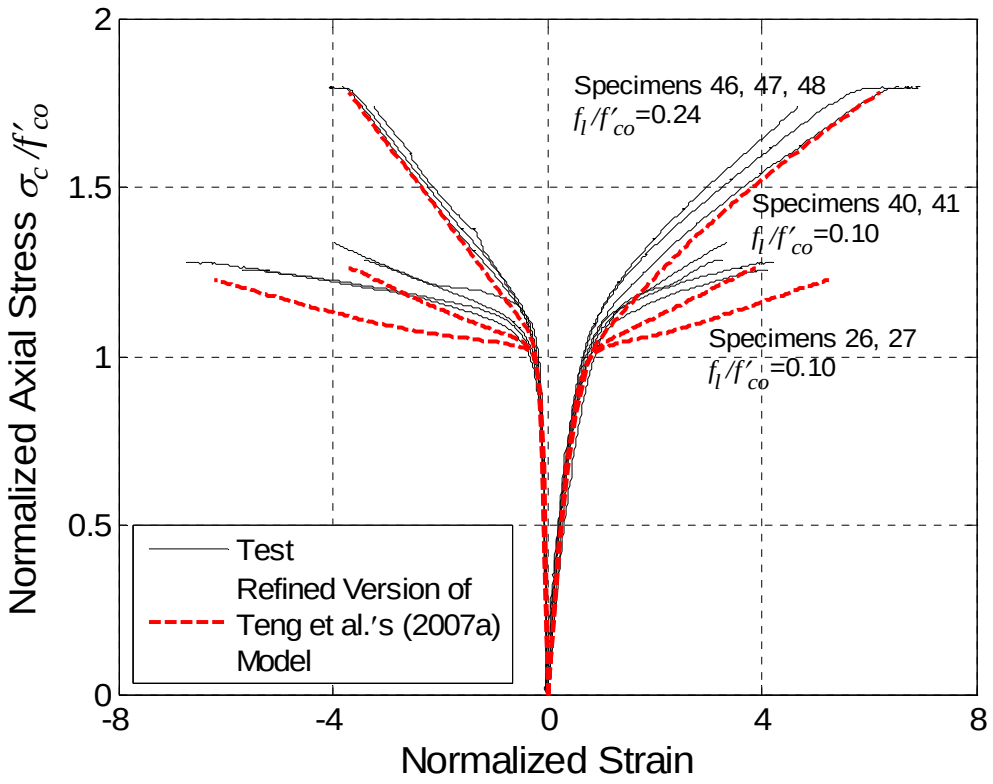

(h) Specimens 26,27; 40,41; 46,47,48

Fig. 1 Stress-strain curves of FRP-confined concrete

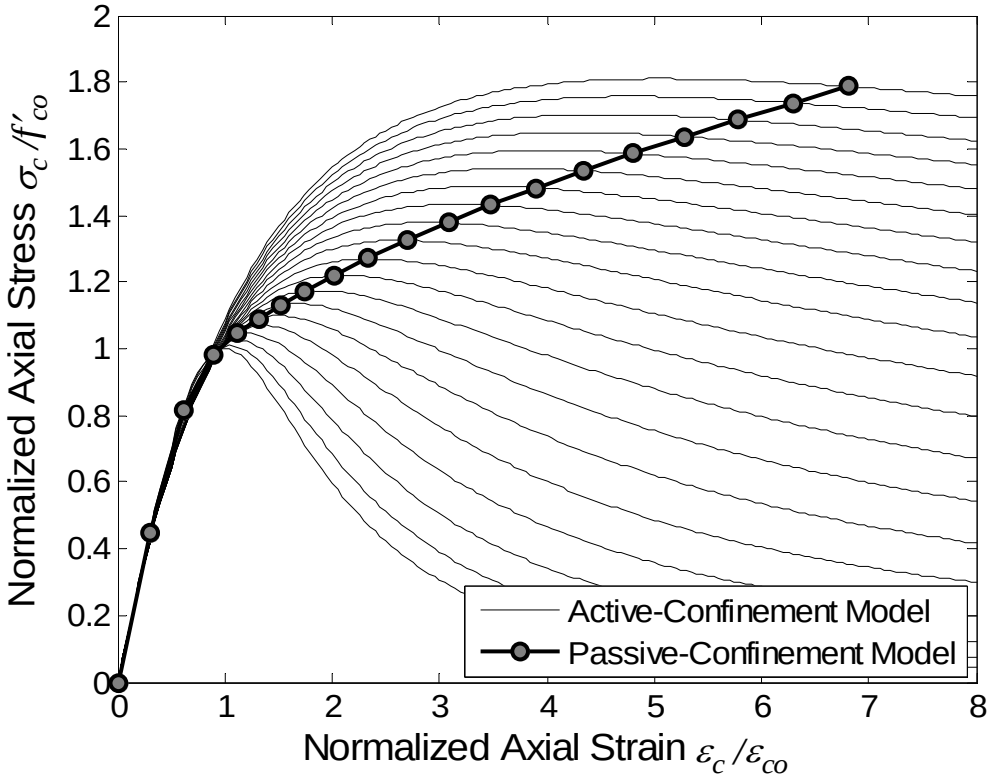

Fig. 2 Generation of a stress-strain curve for FRP-confined concrete

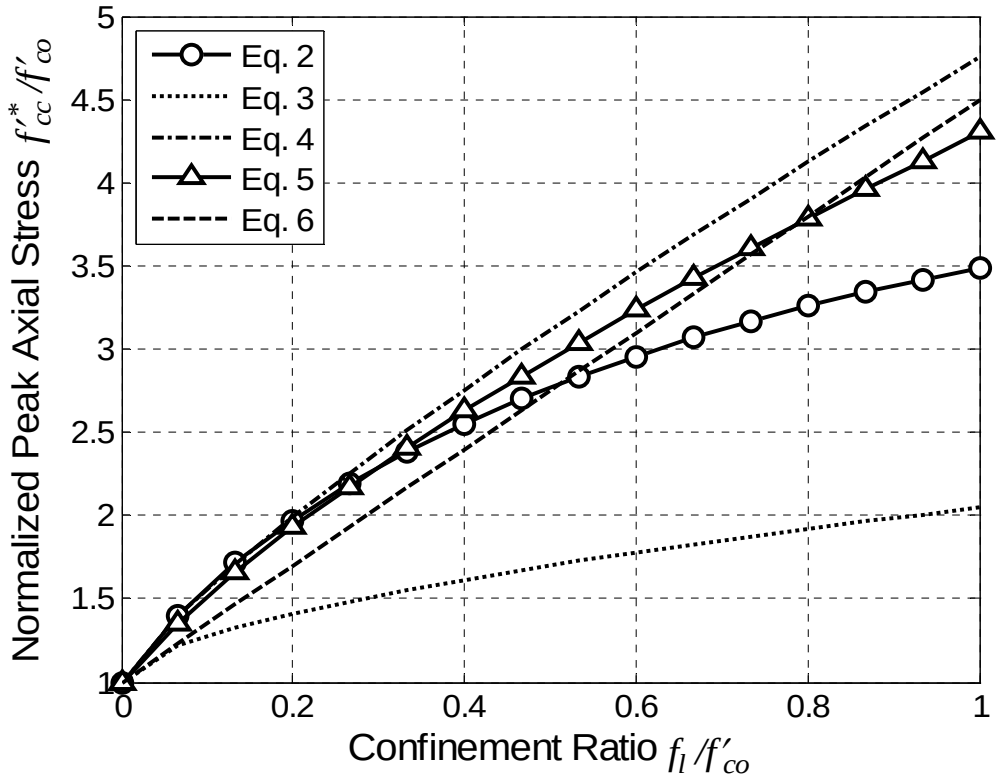

Fig. 3 Comparison of predictions for the peak axial stress

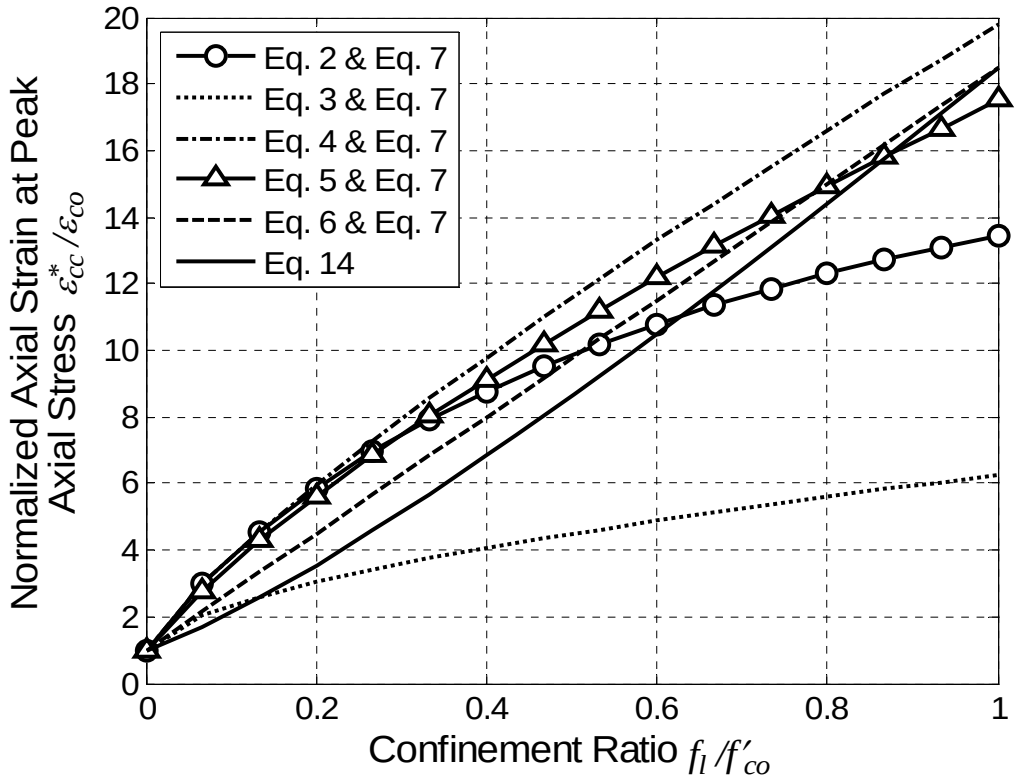

Fig. 4 Comparison of predictions for the axial strain at peak axial stress

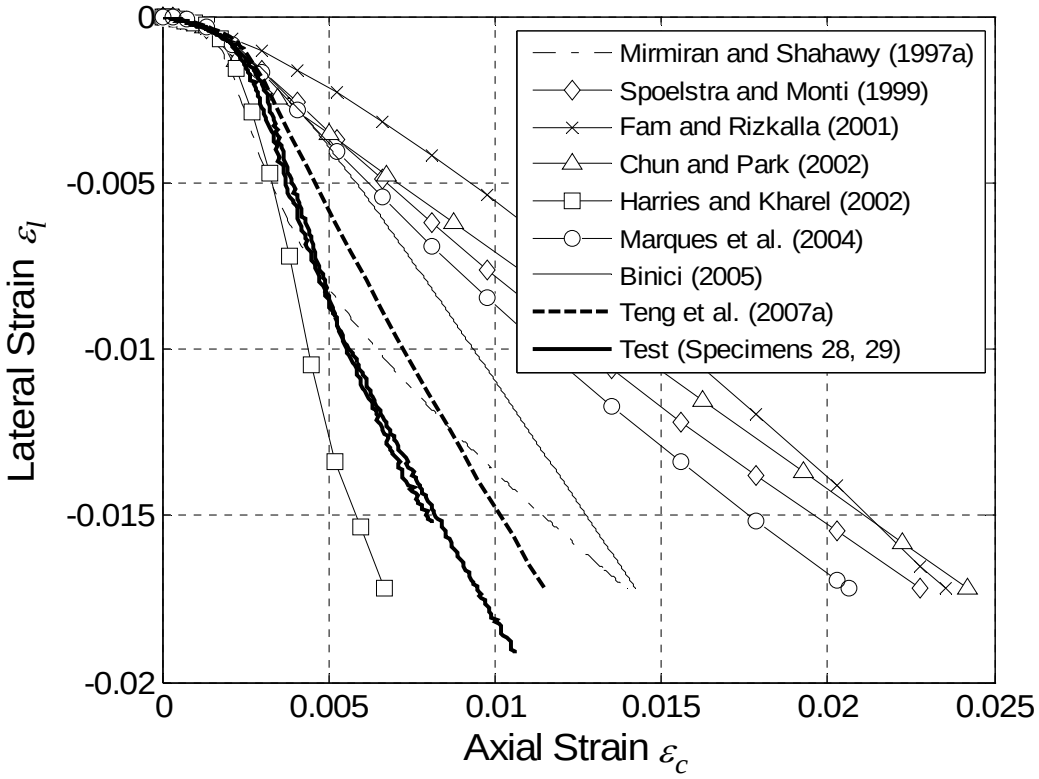

(a) Lateral-to-axial strain curves

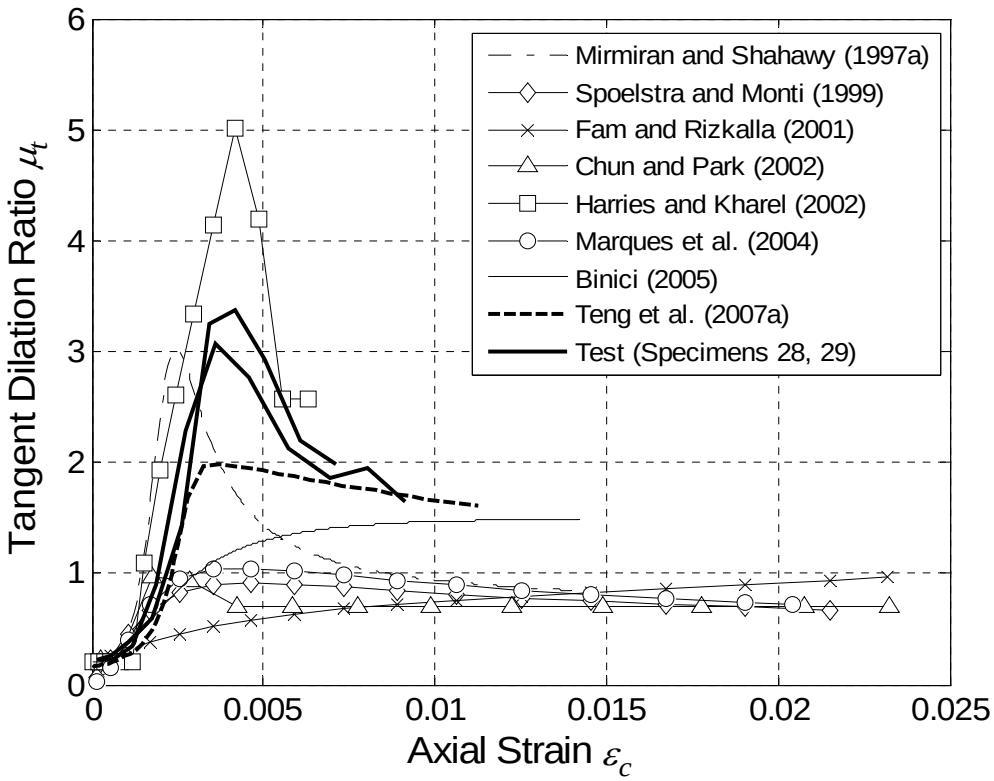

(b) Tangent dilation ratio

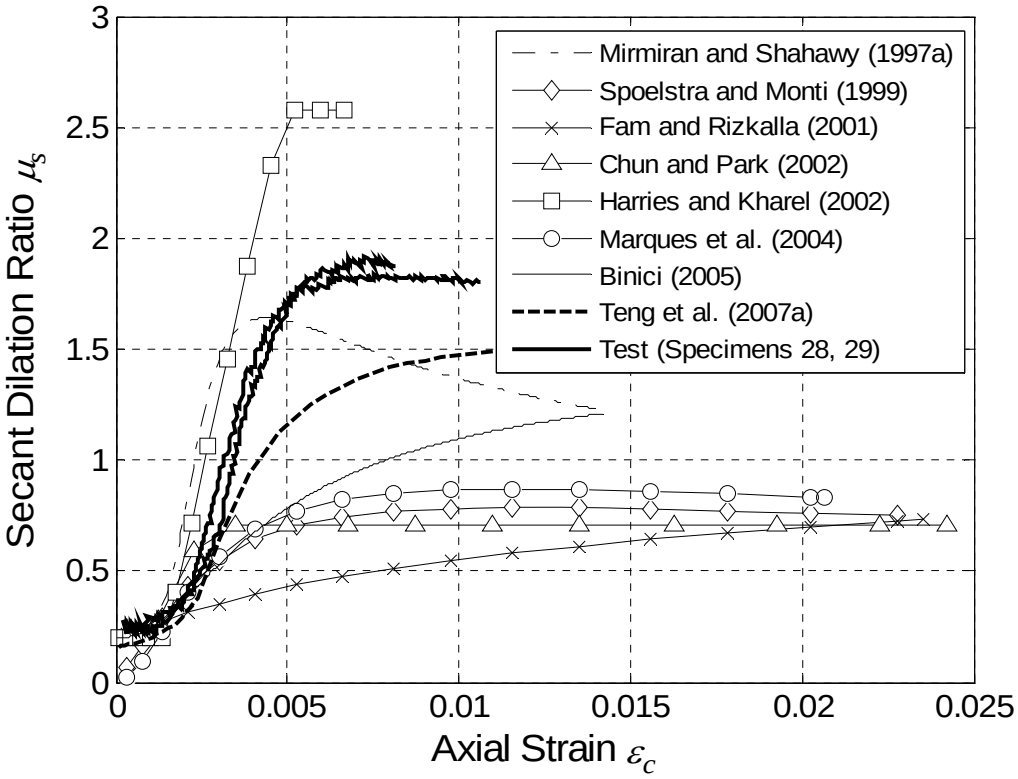

(c) Secant dilation ratio

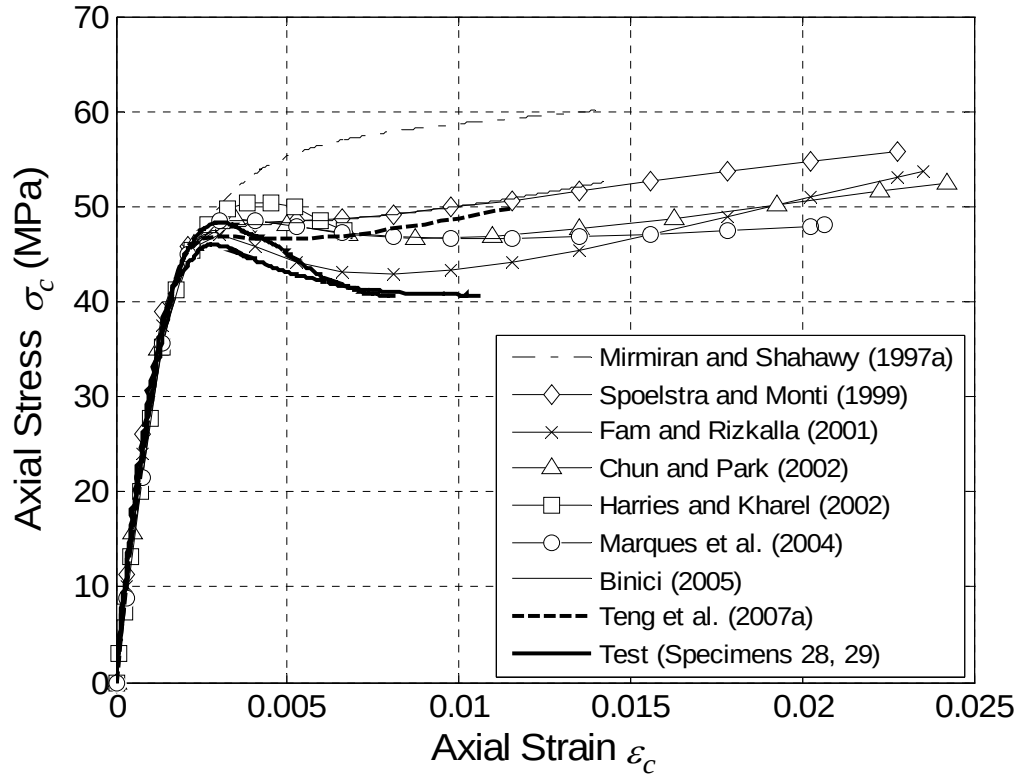

(d) Stress-strain curves

Fig. 5 Weakly-confined concrete

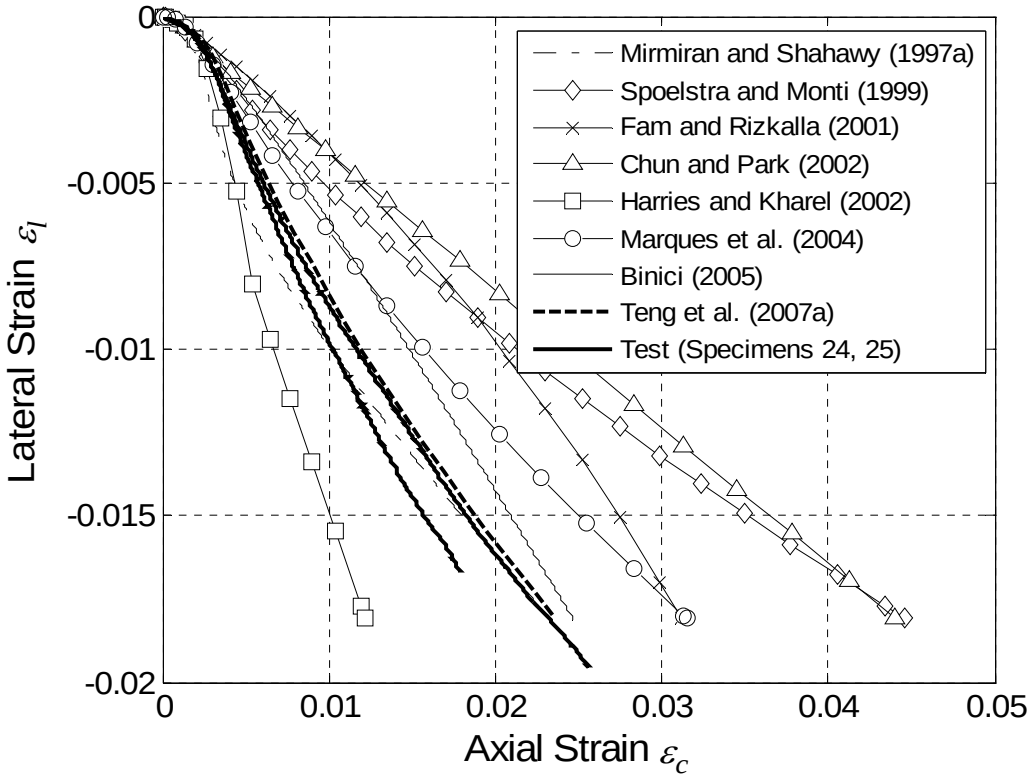

(a) Lateral-to-axial strain curves

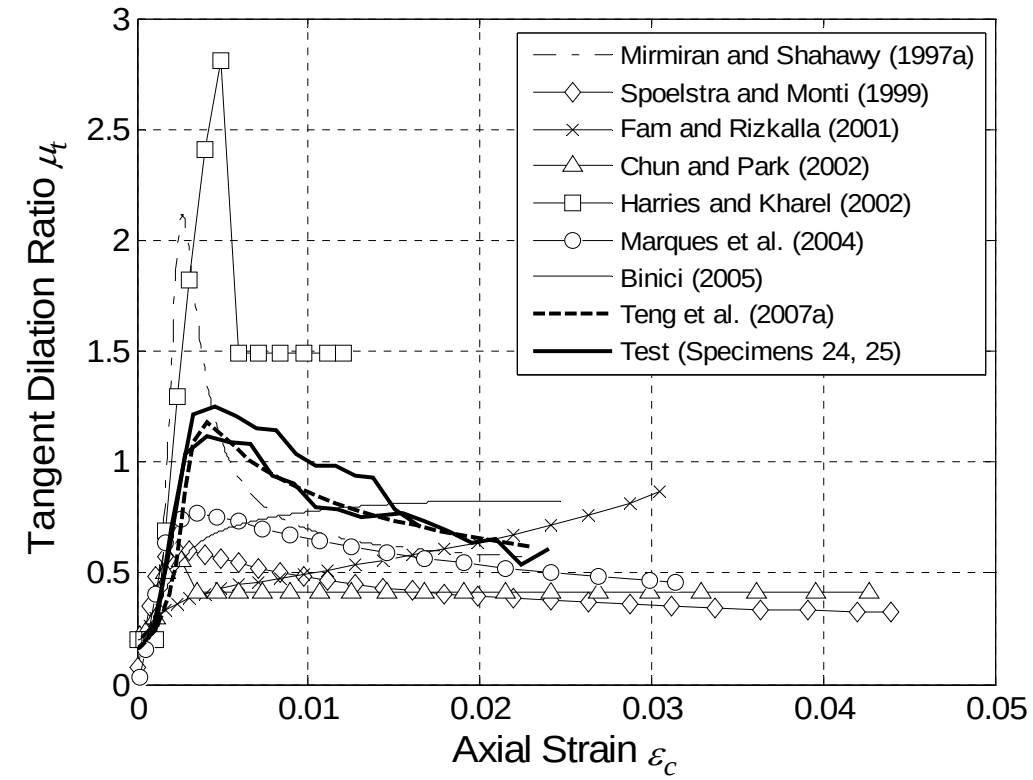

(b) Tangent dilation ratio

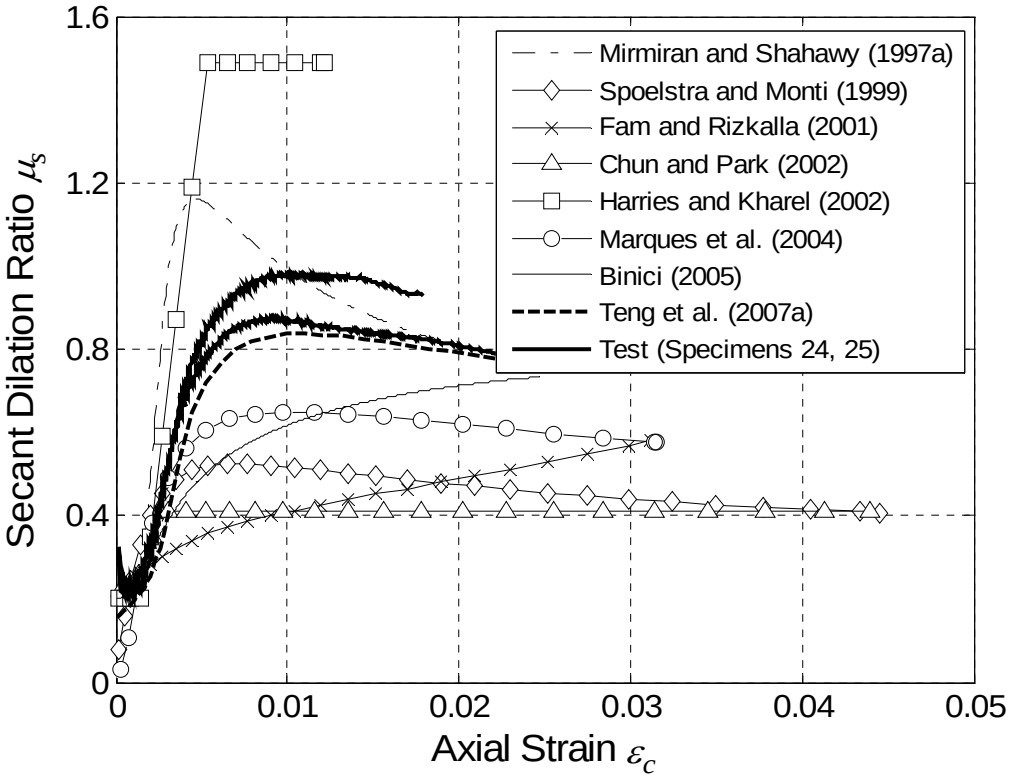

(c) Secant dilation ratio

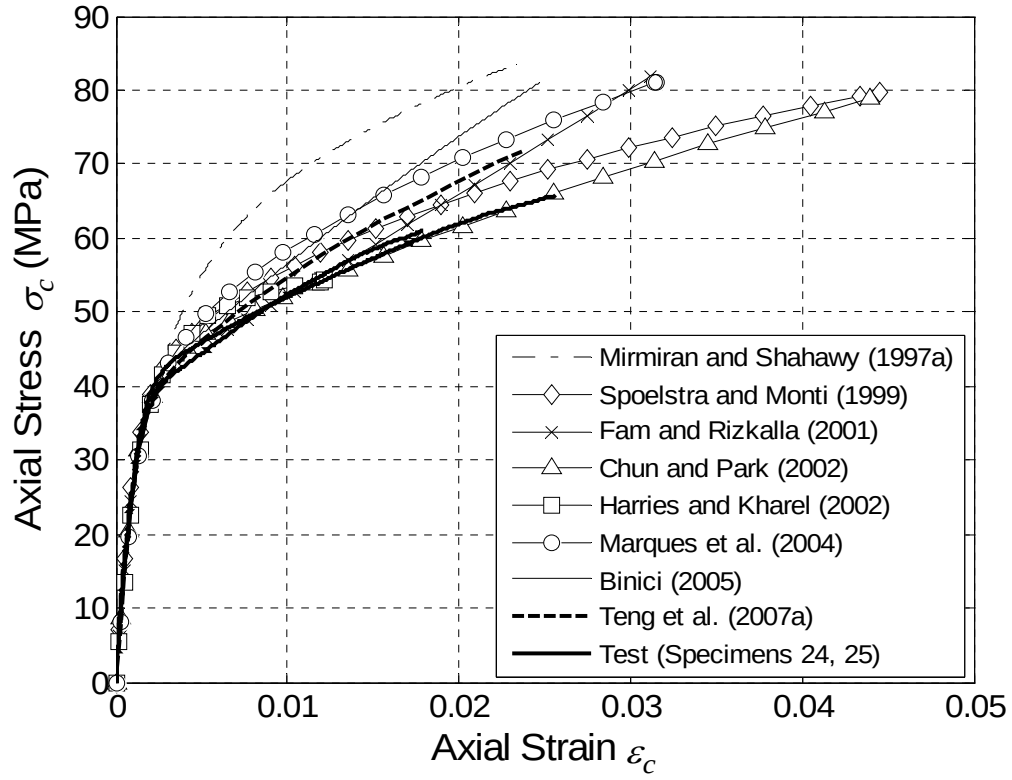

(d) Stress-strain curves

Fig. 6 Moderately-confined concrete

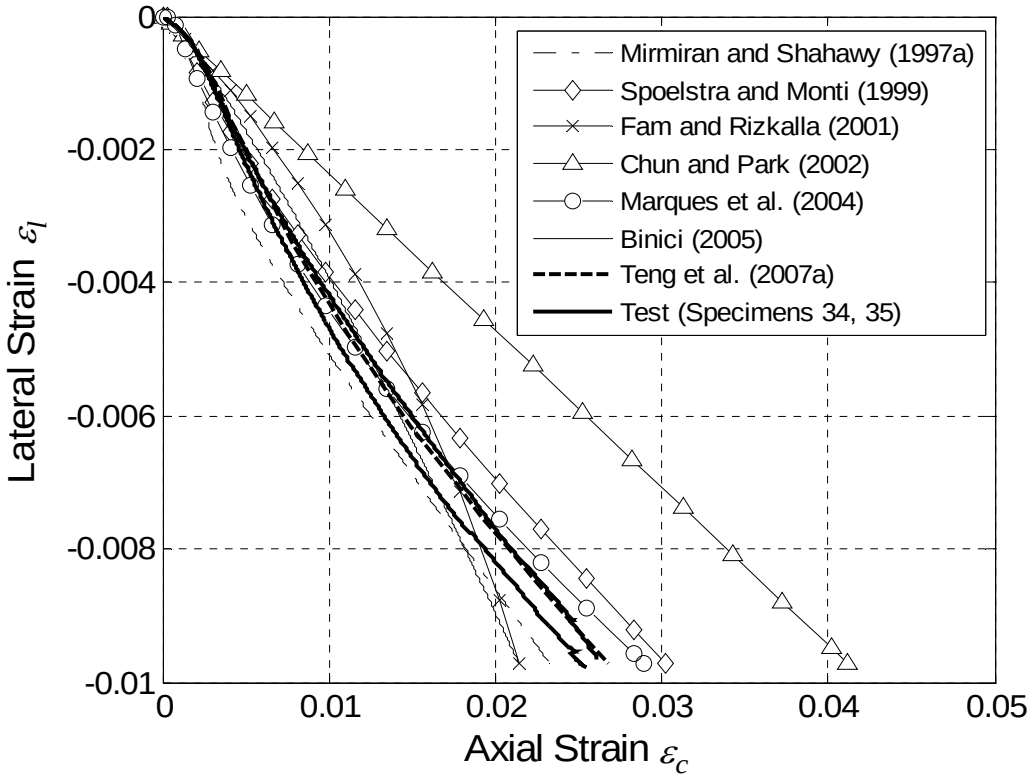

(a) Lateral-to-axial strain curves

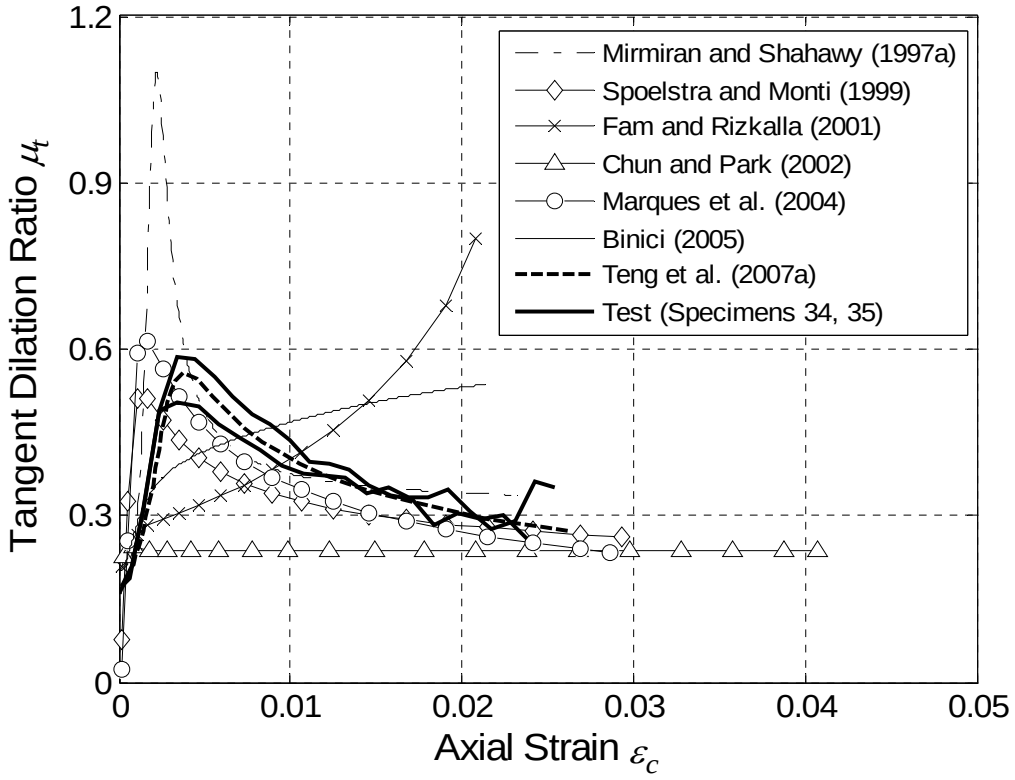

(b) Tangent dilation ratio

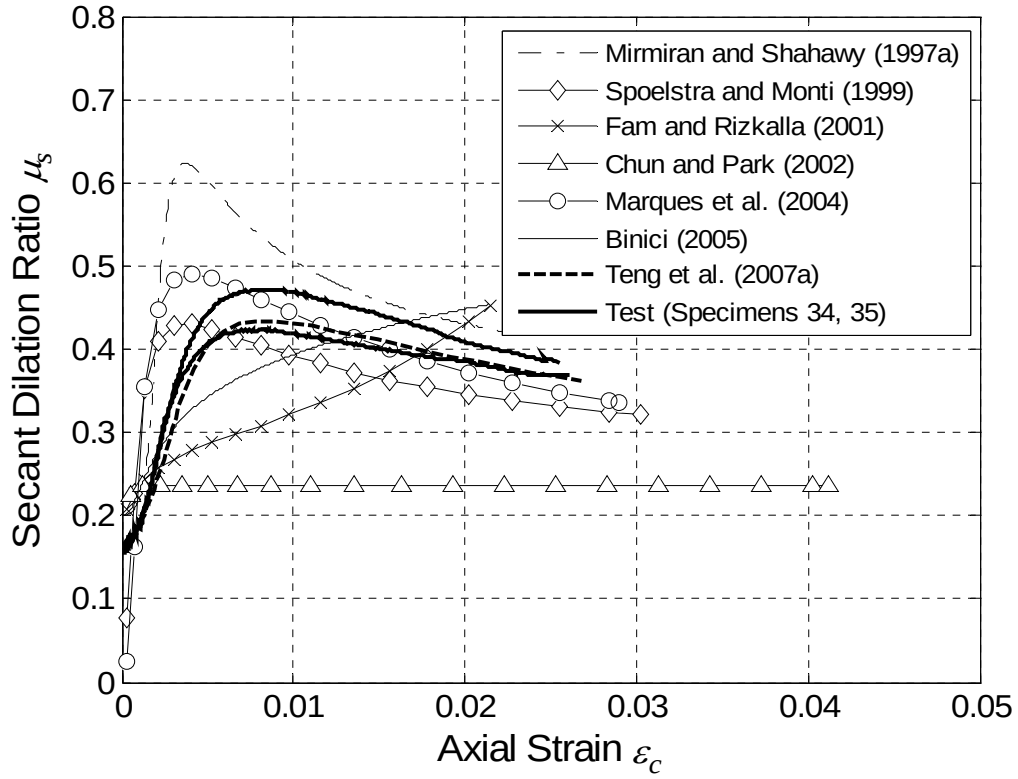

(c) Secant dilation ratio

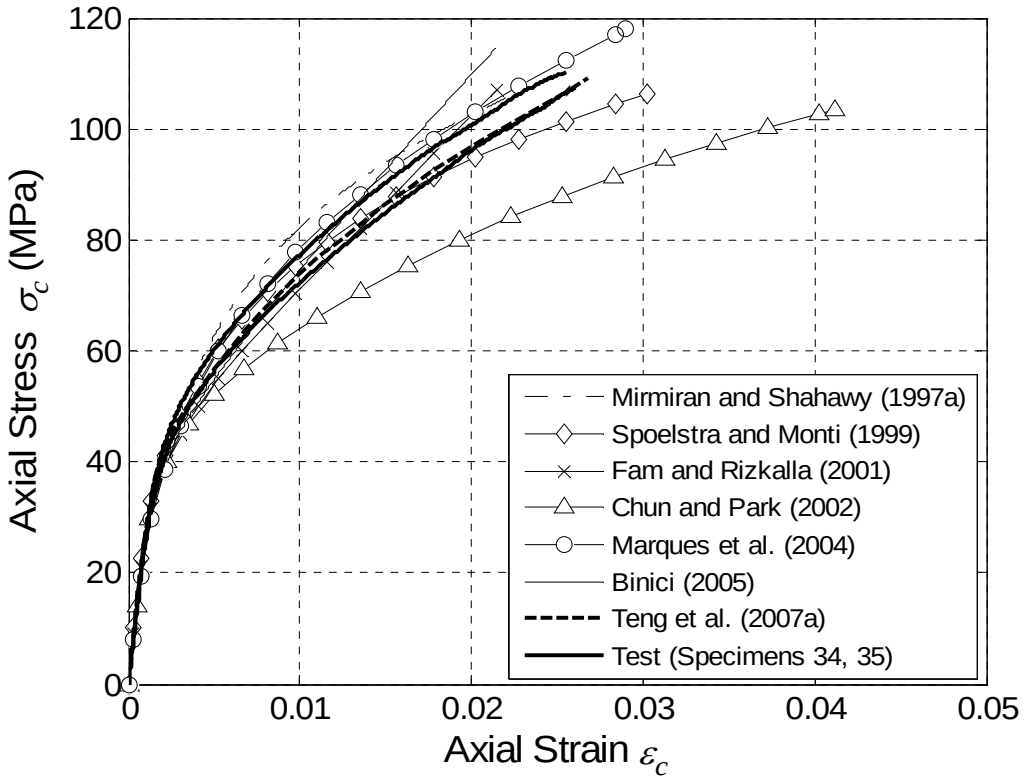

(d) Stress-strain curves

Fig. 7 Heavily-confined concrete

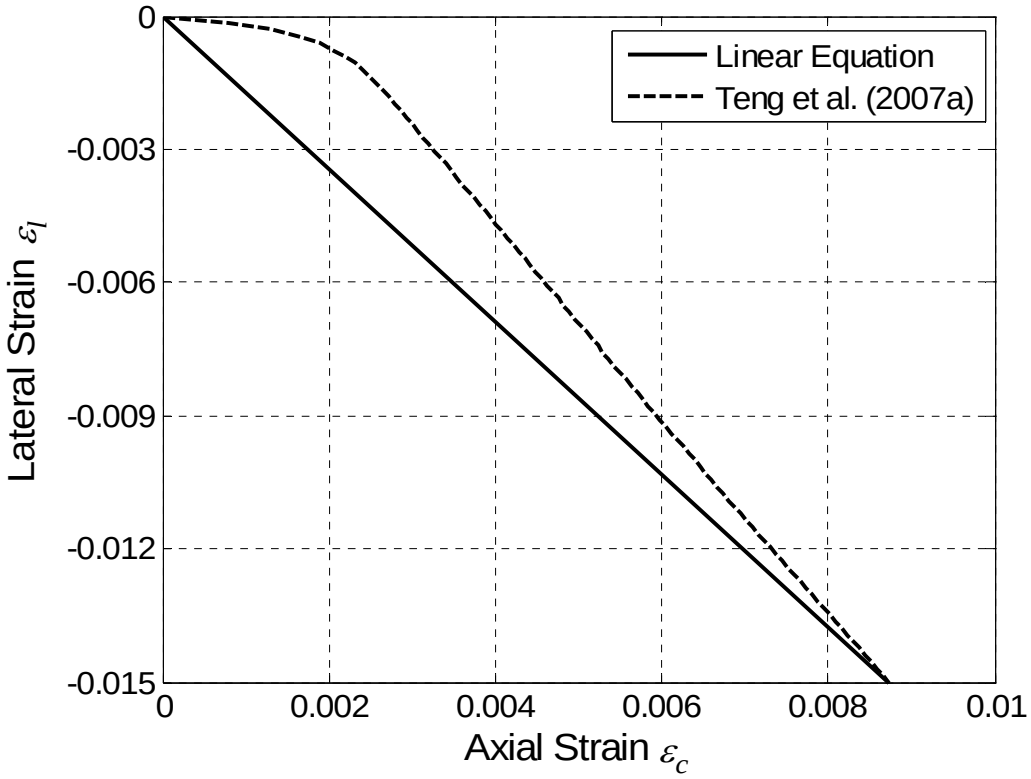

(a) Descending type: lateral-to-axial strain curves

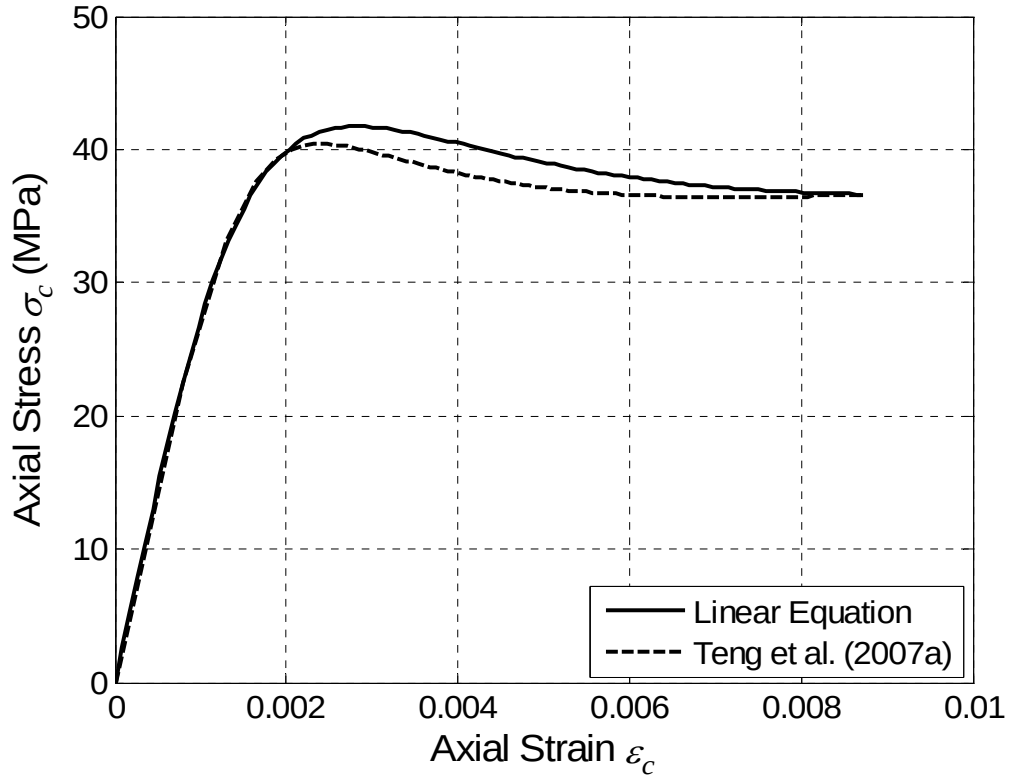

(b) Descending type: stress-strain curves

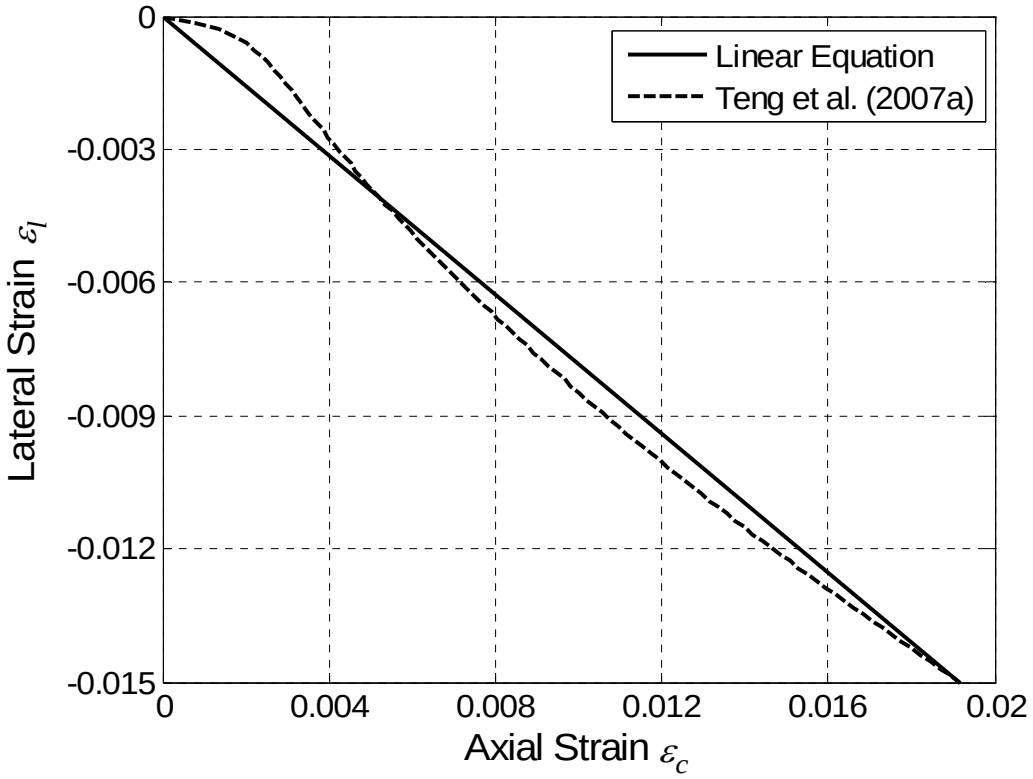

(c) Ascending type: lateral-to-axial strain curves

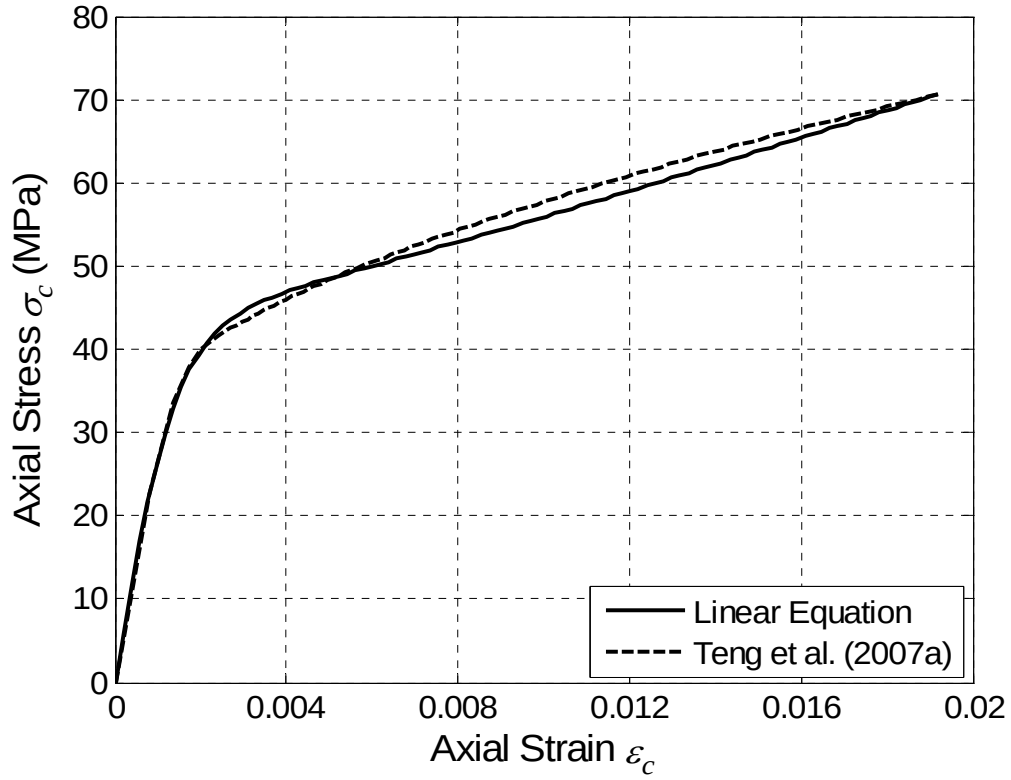

(d) Ascending type: stress-strain curves

Fig. 8 Stress-strain curves predicted by Teng et al.'s (2007a) model: effect of lateral-to-axial strain equation

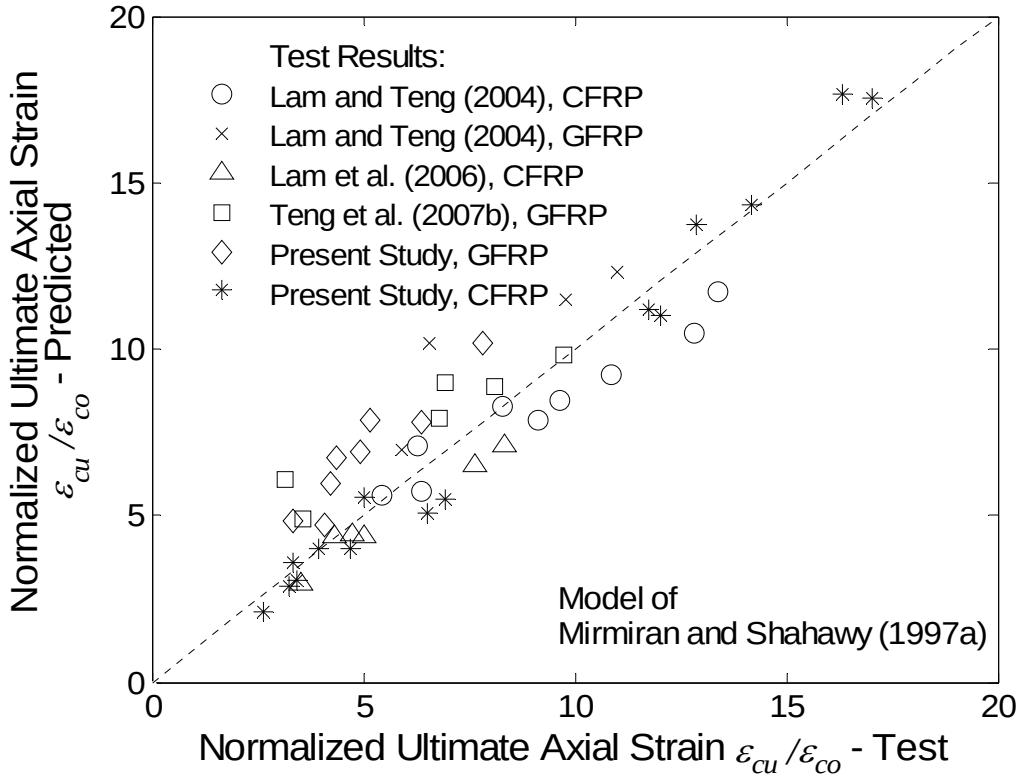

(a) Ultimate axial strain

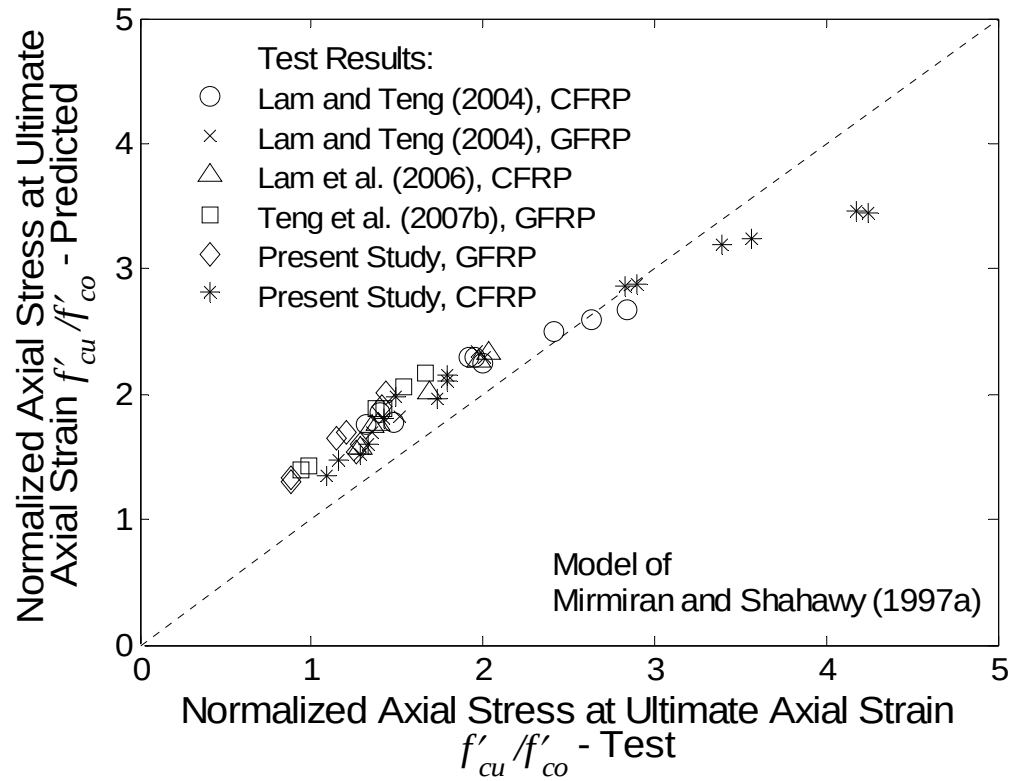

(b) Axial stress at ultimate axial strain

Fig. 9 Performance of Mirmiran and Shahawy's model in predicting the ultimate condition

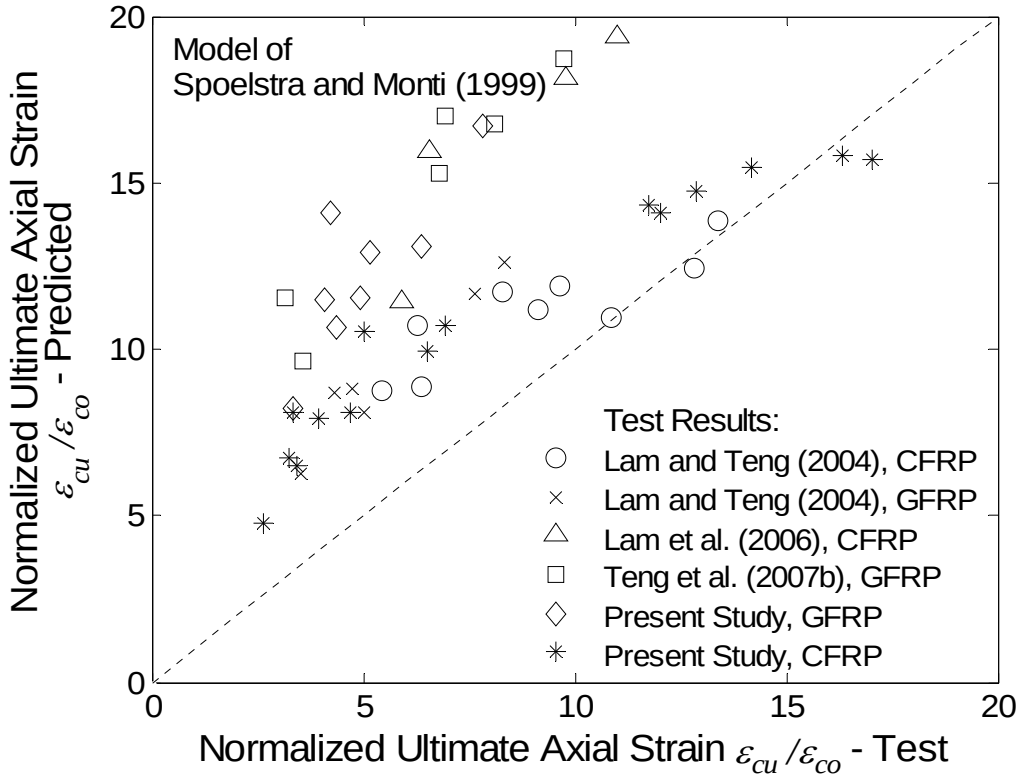

(a) Ultimate axial strain

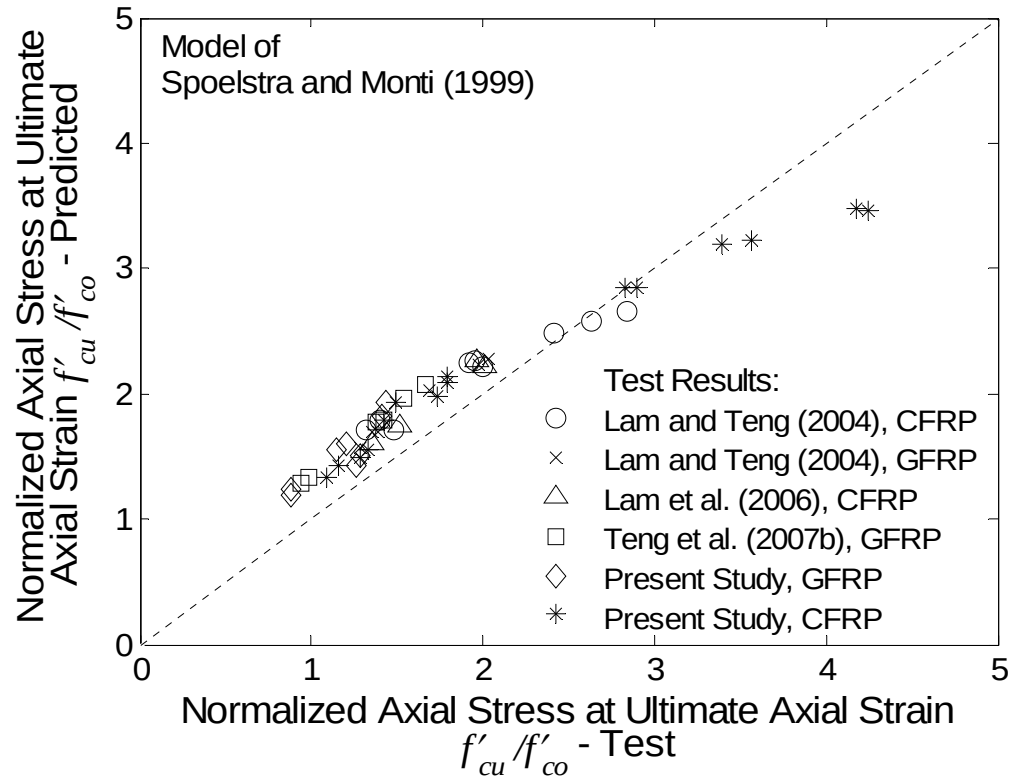

(b) Axial stress at ultimate axial strain

Fig. 10 Performance of Spoelstra and Monti's model in predicting the ultimate condition

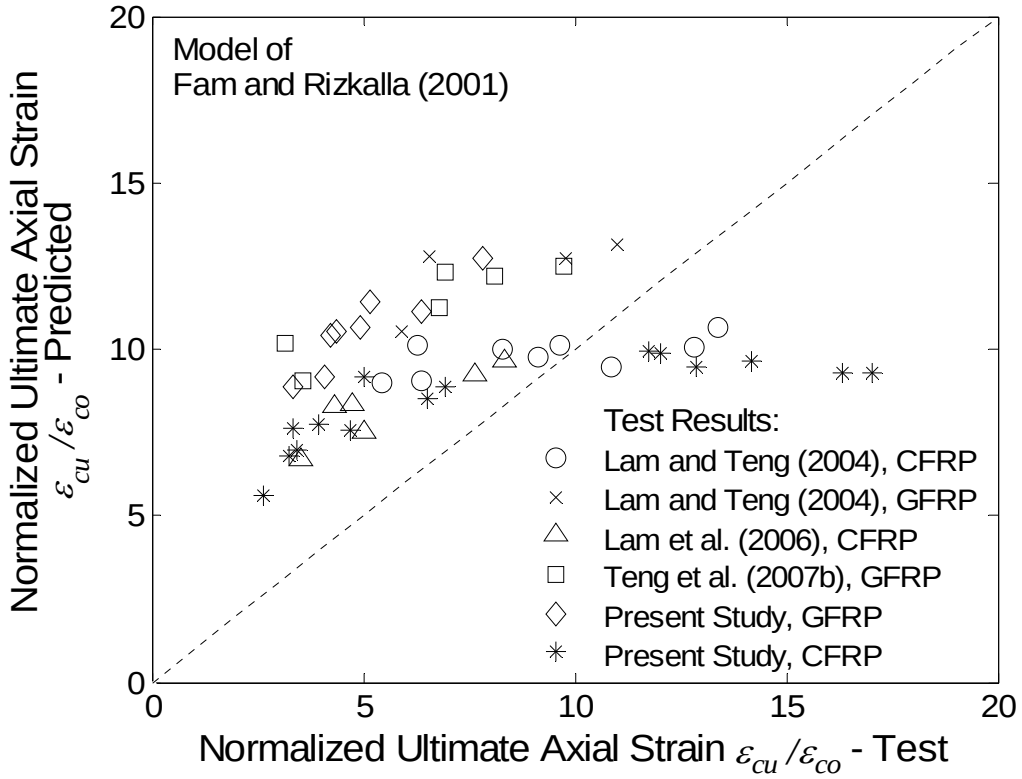

(a) Ultimate axial strain

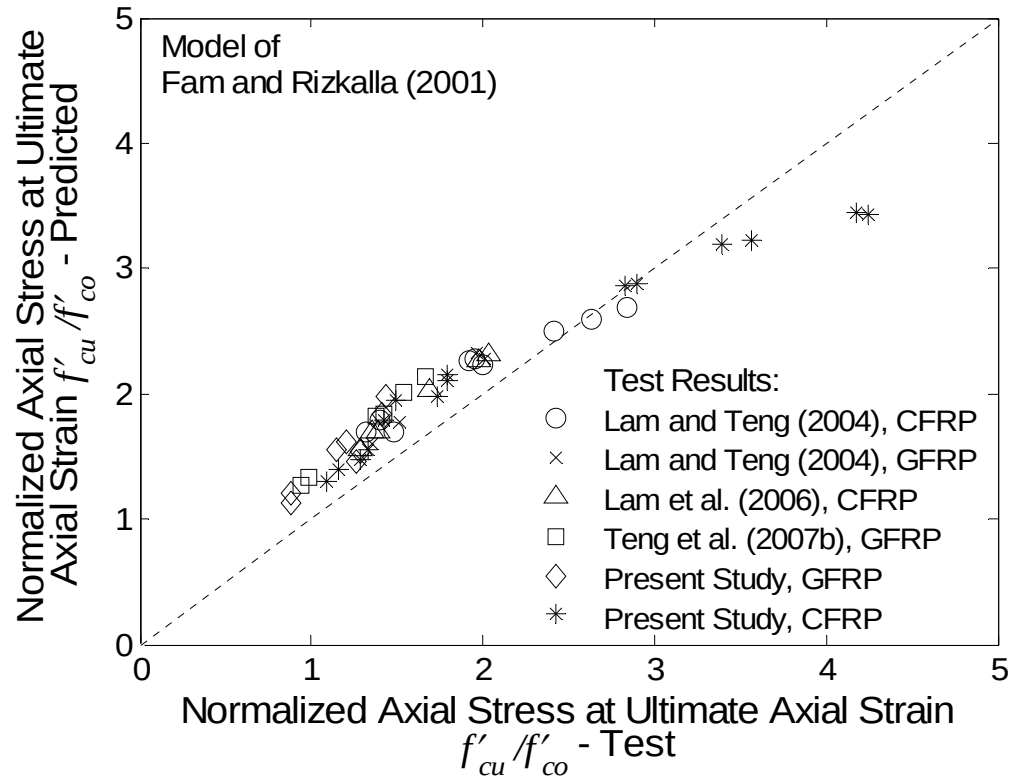

(b) Axial stress at ultimate axial strain

Fig. 11 Performance of Fam and Rizkalla's model in predicting the ultimate condition

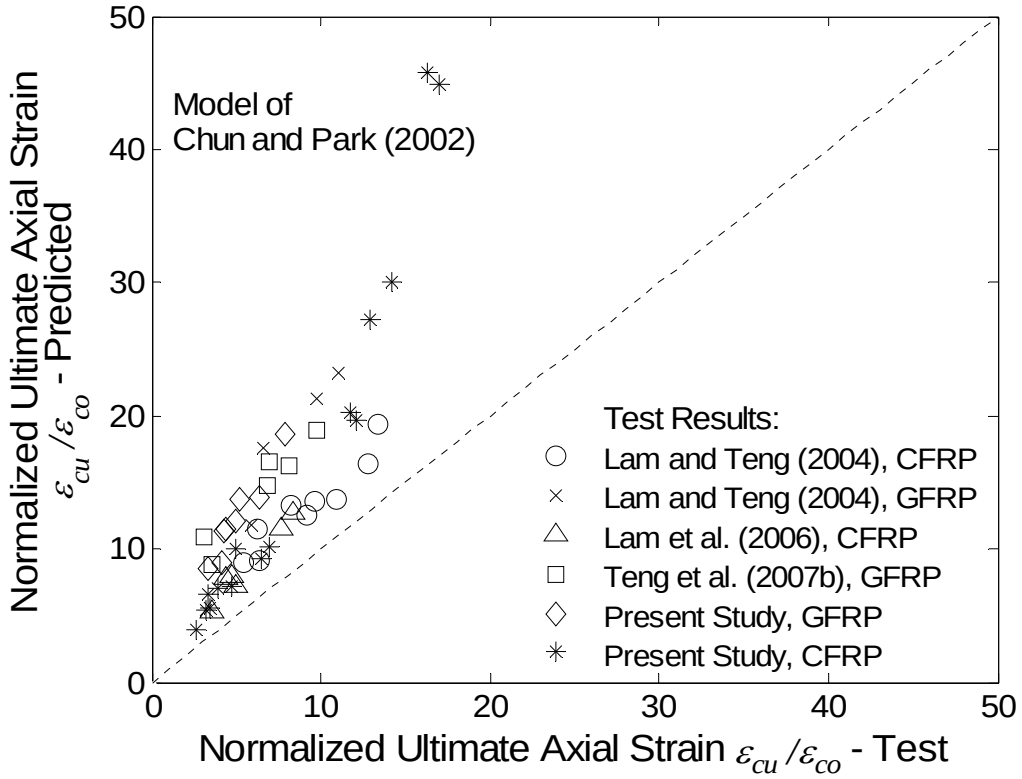

(a) Ultimate axial strain

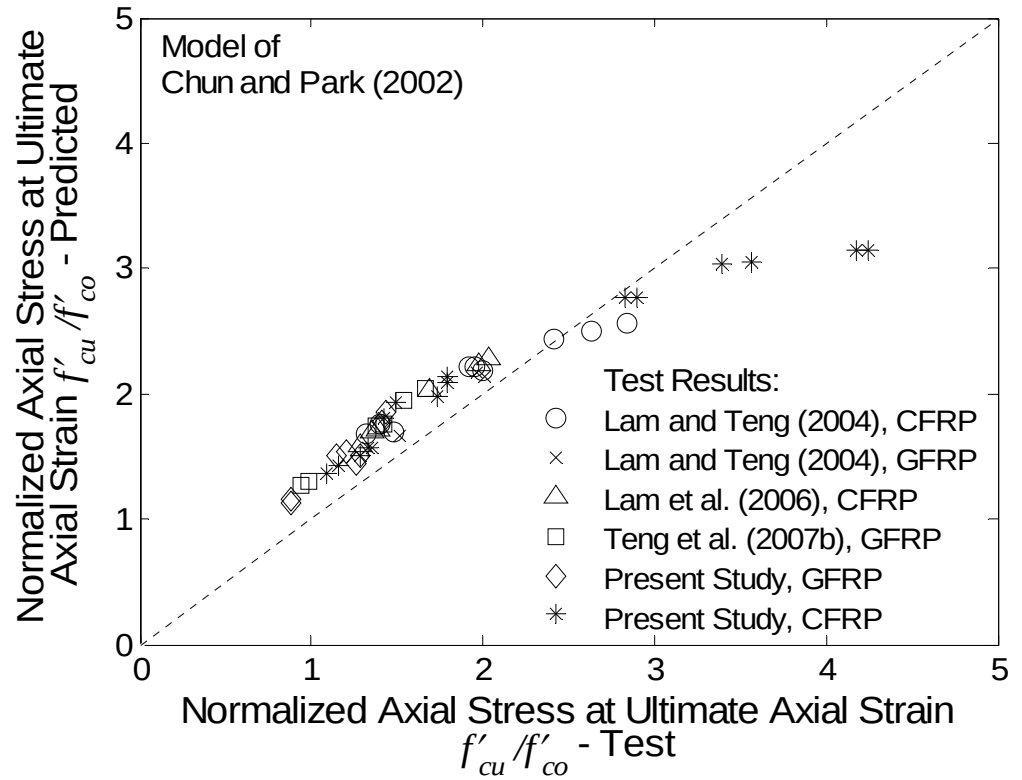

(b) Axial stress at ultimate axial strain

Fig. 12 Performance of Chun and Park's model in predicting the ultimate condition

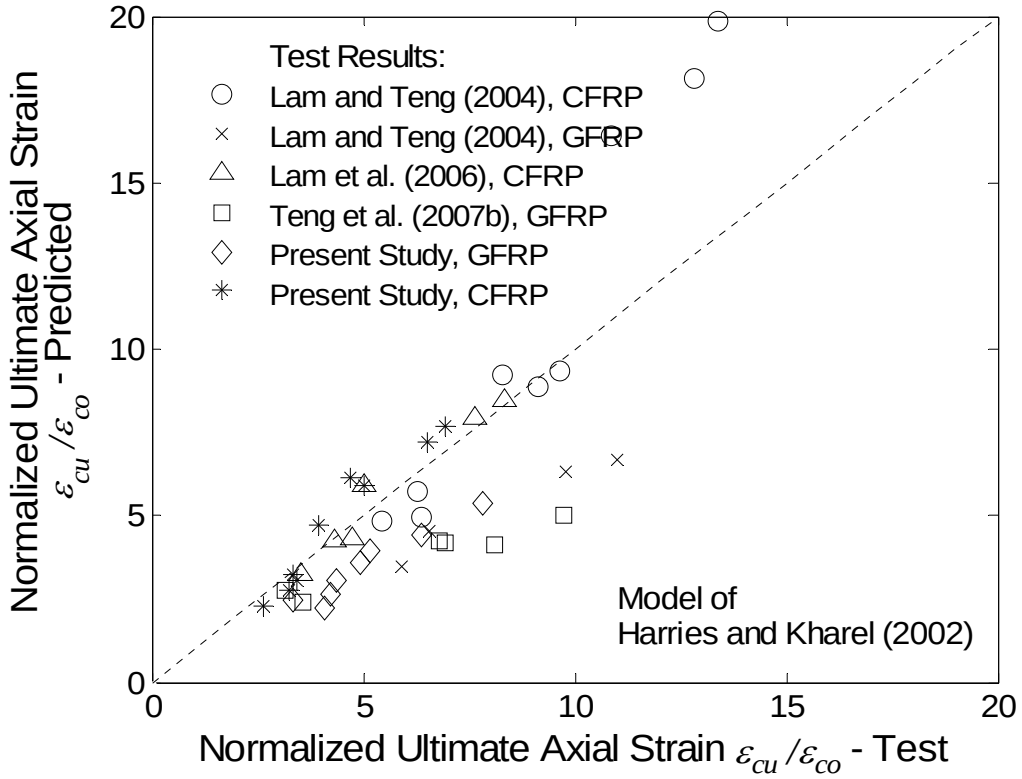

(a) Ultimate axial strain

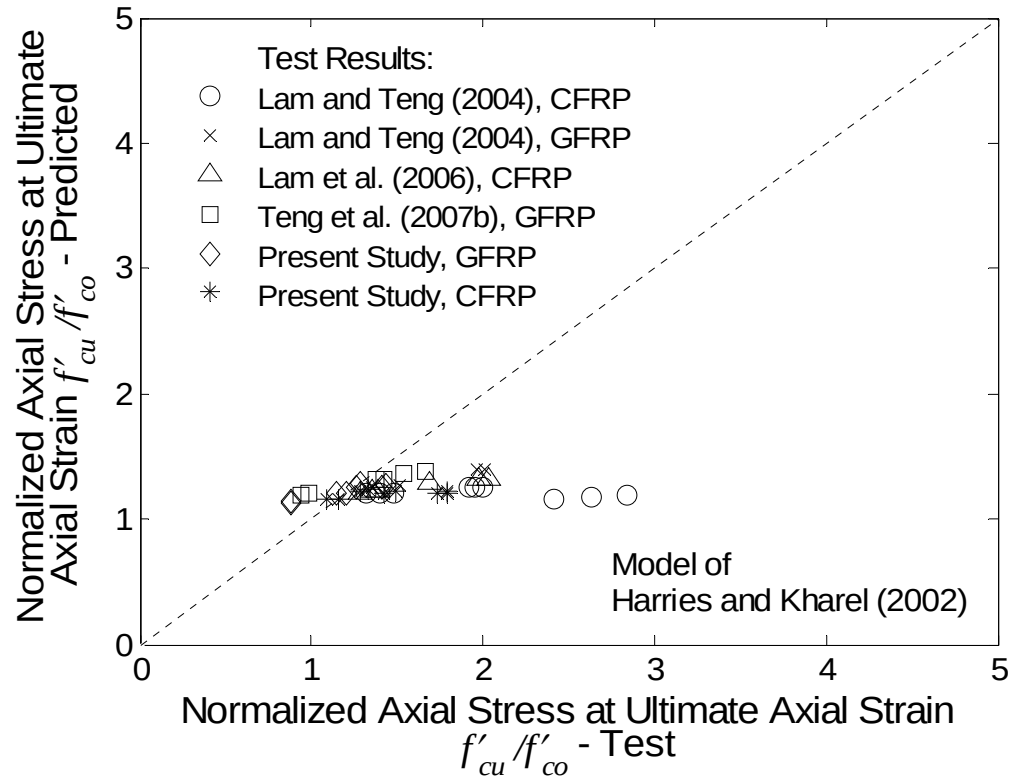

(b) Axial stress at ultimate axial strain

Fig. 13 Performance of Harries and Kharel's model in predicting the ultimate condition

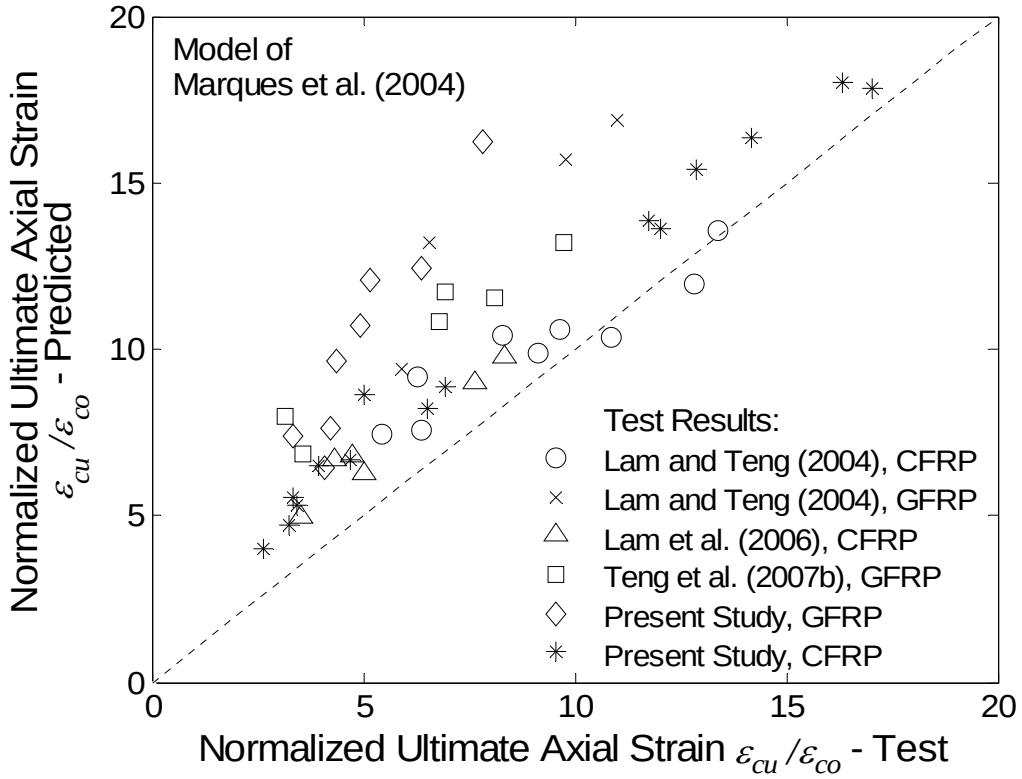

(a) Ultimate axial strain

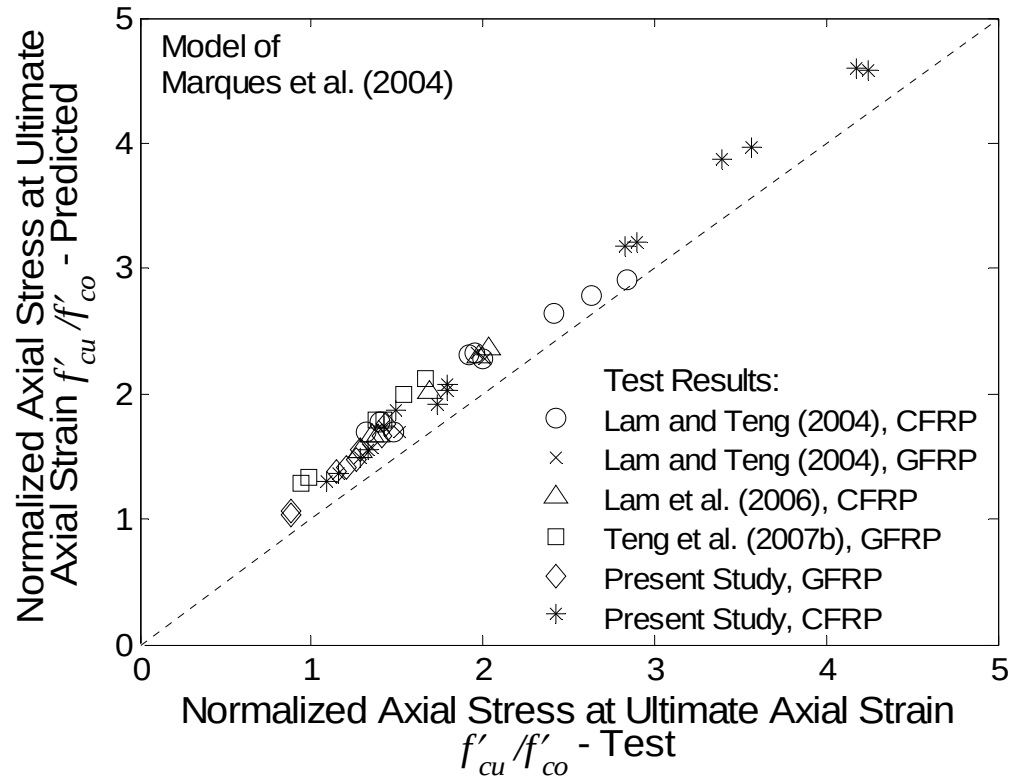

(b) Axial stress at ultimate axial strain

Fig. 14 Performance of Marques et al.'s model in predicting the ultimate condition

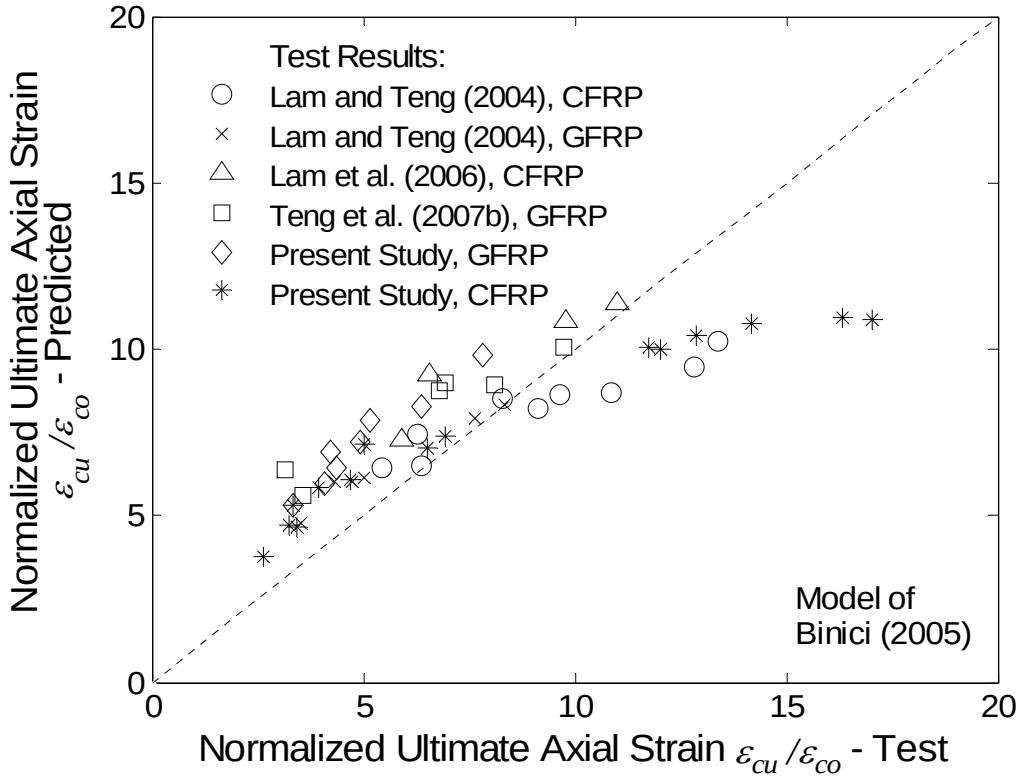

(a) Ultimate axial strain

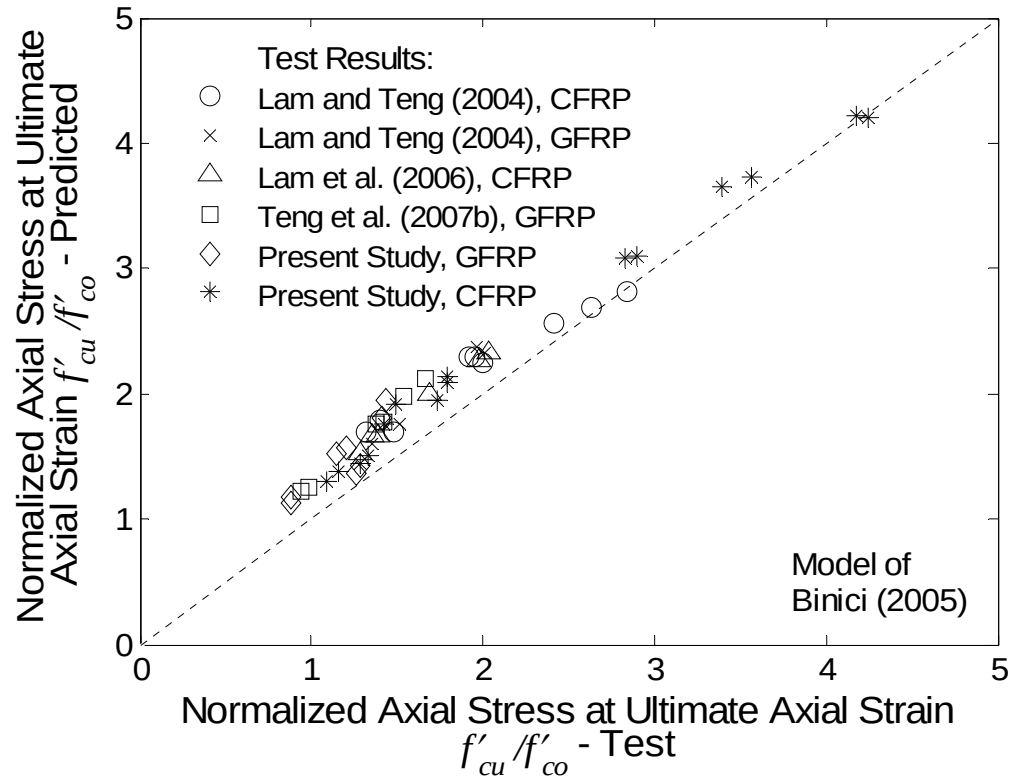

(b) Axial stress at ultimate axial strain

Fig. 15 Performance of Binici's model in predicting the ultimate condition

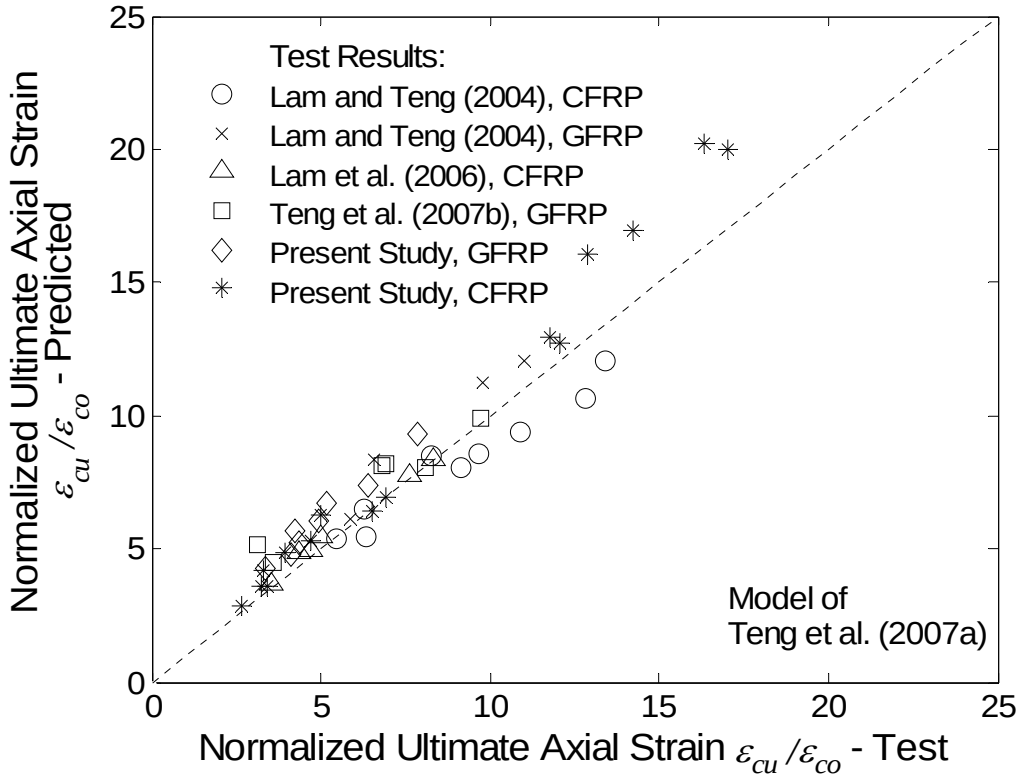

(a) Ultimate axial strain

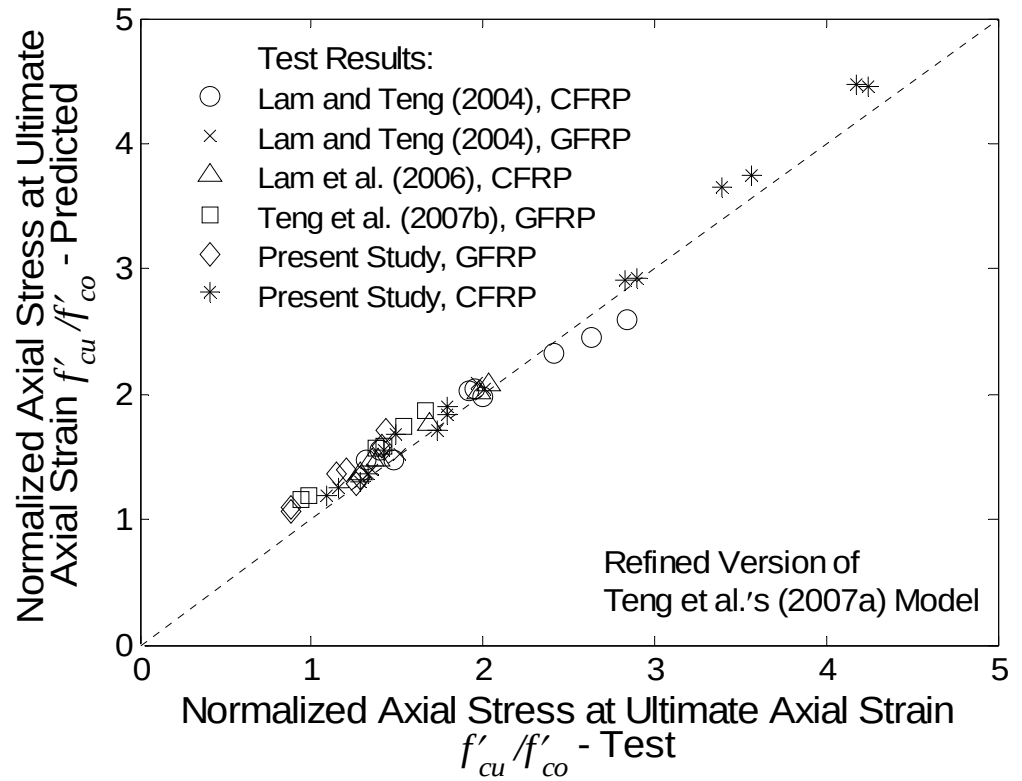

(b) Axial stress at ultimate axial strain

Fig. 16 Performance of Teng et al.'s model in predicting the ultimate condition

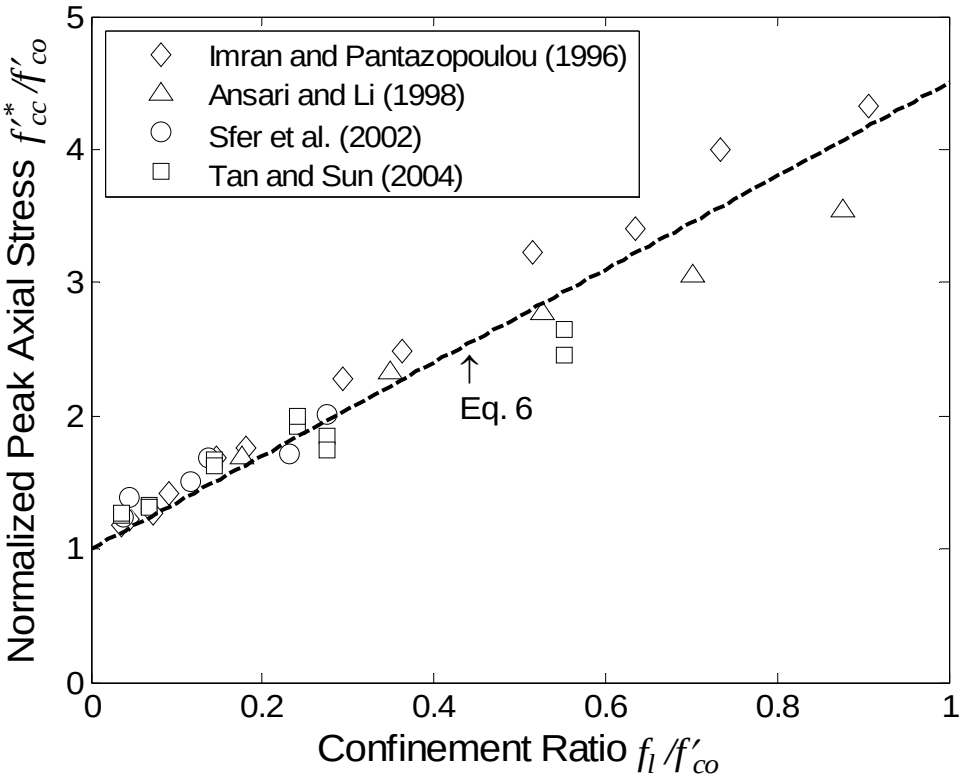

Fig. 17 Normalized peak axial stress versus confinement ratio

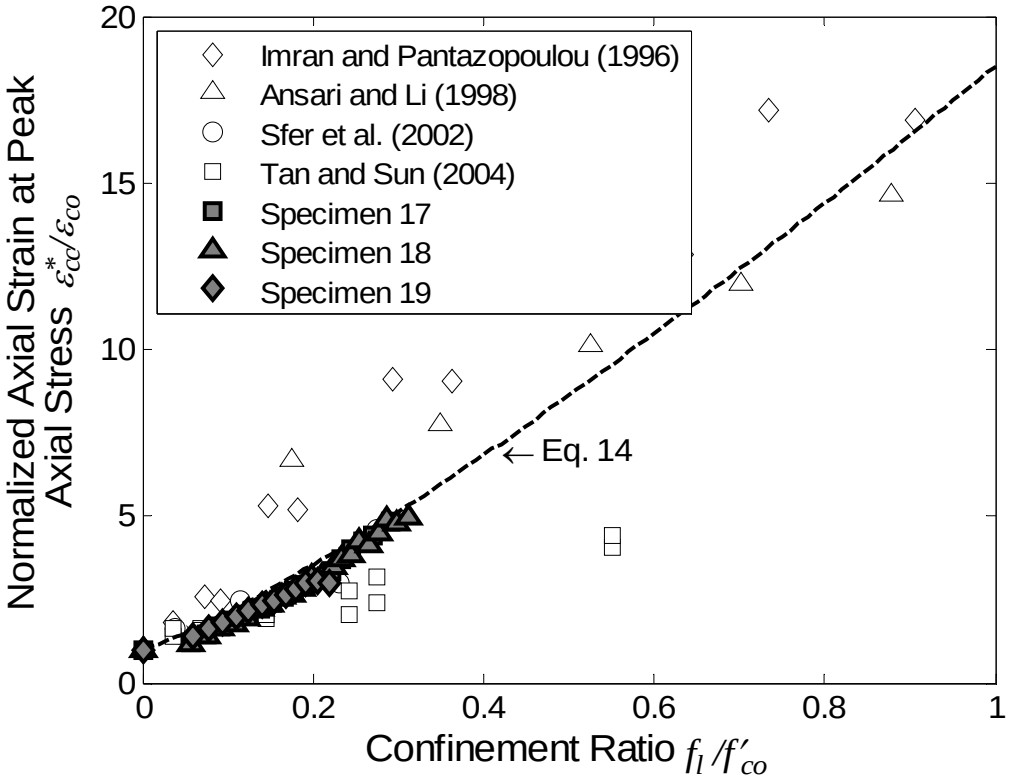

Fig. 18 Normalized axial strain at peak axial stress versus confinement ratio

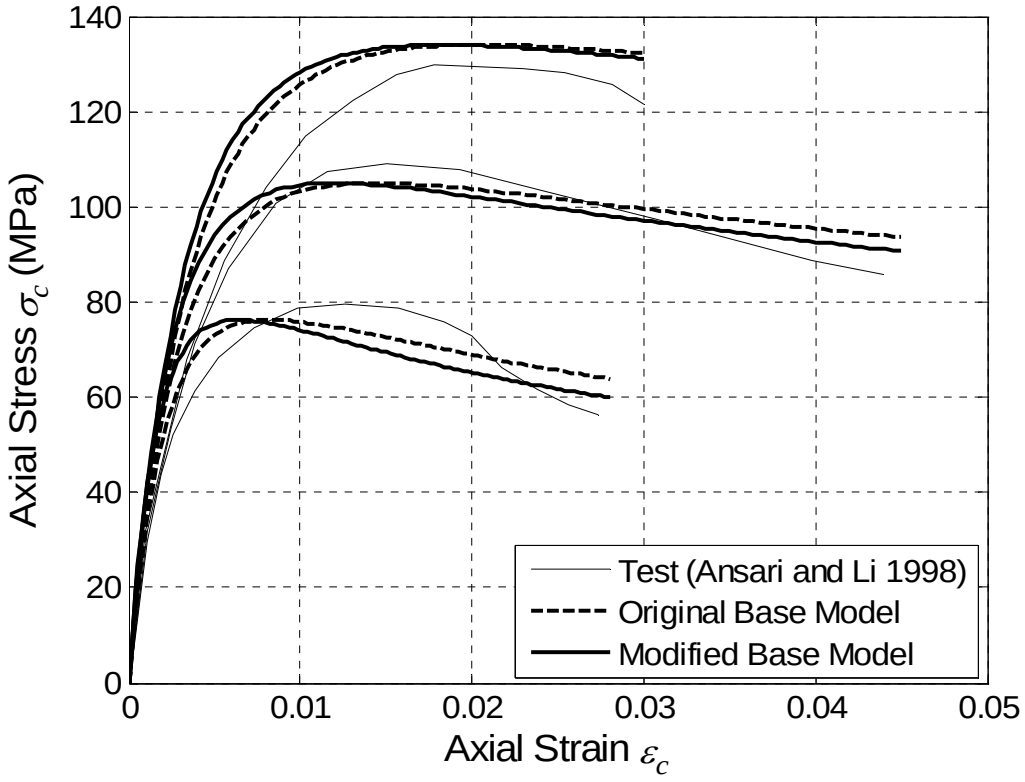

Fig. 19 Comparisons of original base model with modified base model

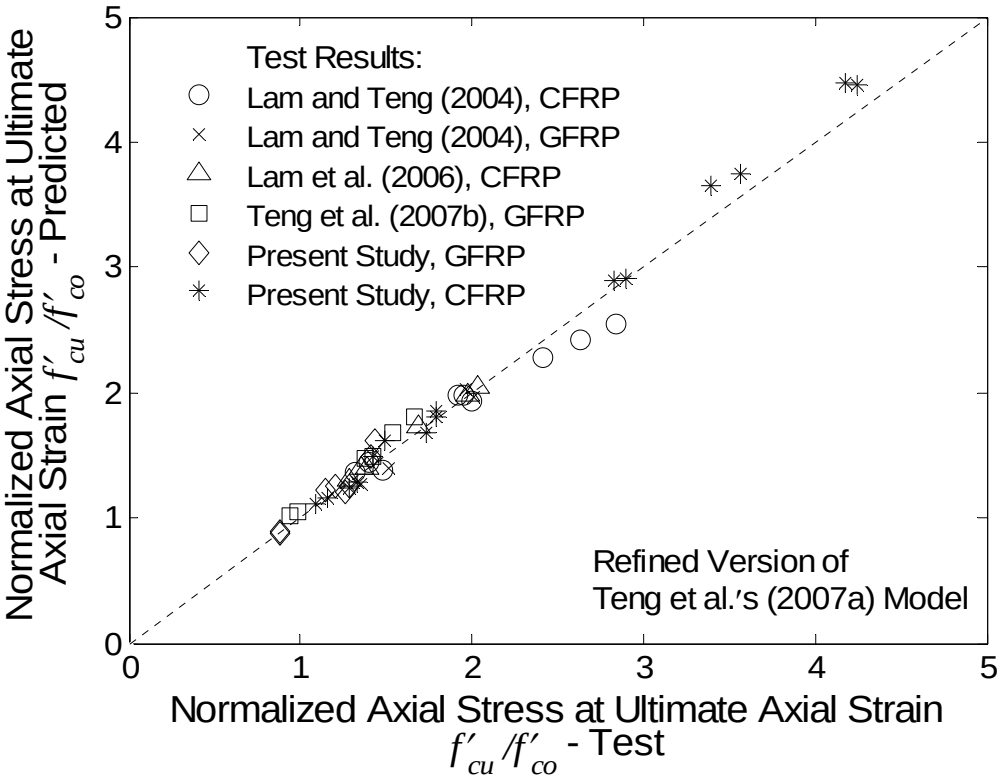

Fig. 20 Performance of refined version of Teng et al.'s model